

CO-AGGREGATION OF THE PROTEINS TRIOBP-1 AND NDE1, AND THEIR RELEVANCE TO MENTAL ILLNESS

Hart, Anja

Master's thesis / Diplomski rad

2023

Degree Grantor / Ustanova koja je dodijelila akademski / stručni stupanj: **University of Rijeka / Sveučilište u Rijeci**

Permanent link / Trajna poveznica: <https://urn.nsk.hr/urn:nbn:hr:193:466940>

Rights / Prava: [In copyright](#) / [Zaštićeno autorskim pravom.](#)

Download date / Datum preuzimanja: **2024-05-23**

Repository / Repozitorij:



[Repository of the University of Rijeka, Faculty of Biotechnology and Drug Development - BIOTECHRI Repository](#)



UNIVERSITY OF RIJEKA
DEPARTMENT OF BIOTECHNOLOGY
Graduate university programme
Biotechnology in Medicine

Anja Hart

**CO-AGGREGATION OF THE PROTEINS TRIOBP-1 AND
NDE1, AND THEIR RELEVANCE TO MENTAL ILLNESS**

Master's thesis

Rijeka, 2023

UNIVERSITY OF RIJEKA
DEPARTMENT OF BIOTECHNOLOGY
Graduate university programme
Biotechnology in Medicine

Anja Hart

**CO-AGGREGATION OF THE PROTEINS TRIOBP-1 AND
NDE1, AND THEIR RELEVANCE TO MENTAL ILLNESS**

Master's thesis

Rijeka, 2023

Mentor: izv.prof.dr.sc. Nicholas J. Bradshaw

SVEUČILIŠTE U RIJECI
ODJEL ZA BIOTEHNOLOGIJU
Diplomski sveučilišni studij
Biotehnologija u medicini

Anja Hart

**KO-AGREGACIJA PROTEINA TRIOBP-1 I NDE1 TE NJIHOVA
ZNAČAJNOST U MENTALNIM BOLESTIMA**

Diplomski rad

Rijeka, 2023.

Mentor: izv.prof.dr.sc. Nicholas J. Bradshaw

Acknowledgements

First, I would like to extend my heartfelt gratitude to my mentor, Nicholas J. Bradshaw, who has been an incredible guide and support throughout my academic path. His patience, advice, and motivating presence keep proving that choosing him as my mentor was the best choice I could have made.

I am really grateful for my lab mates, Bobana, Beti, and Mario, who have become more than just colleagues - they are wonderful friends. Their friendship, help, and encouragement have meant so much to me, both in the lab and outside. Our shared experiences have created a positive and supportive atmosphere that has enriched my academic experience.

I also want to thank my close friends, Tina and Lorena. Our friendship, shared moments, and laughter have been a source of happiness throughout my five years in college. Your support has shown me that facing challenges is easier when you have caring friends by your side.

Last but not least, I want to thank my mom and my brother. Your endless love, guidance, and patience have been my main source of strength. The support and encouragement you were giving have meant the world to me, and I am grateful for everything you've done.

Thank you all for always believing in me and being there for me.

The graduate final thesis was defended on September 27th, 2023.

In front of the Committee:

1. Prof. dr. sc. Miranda Mladinić Pejatović
2. Prof. dr. sc. Mladen Merćep
3. Associate Prof. Nicholas J. Bradshaw

This thesis has pages 66, 17 figures, 8 tables, and 47 citations.

Abstract

Schizophrenia is a chronic mental illness, that affects people worldwide, and presents a significant challenge within the field of mental health. Because of its global rise in prevalence, the imperative to comprehend its underlying molecular mechanisms becomes increasingly vital. The complexity of this and other chronic mental illnesses presents significant diagnostic and treatment challenges, emphasizing the need for innovative approaches to address their intricate nature. Recent insights, as well as the focus of this thesis, aim to shed light on the occurrence of protein aggregation in the context of schizophrenia, offering new perspectives alongside genetics and environmental factors. This thesis focuses on the co-aggregation of TRIOBP-1 and NDE1, both of which play crucial roles in cellular processes and neurobiology and delves into their interaction, aiming to unravel their contributions to the disorder. Previous studies acknowledge NDE1's interactions with aggregating proteins like TRIOBP-1 and DISC1, underscoring its significance in this context.

To investigate this co-aggregation further, we employed a range of methodologies. Plasmids were expressed in neuroblastoma cells, and their interactions were visualized using immunofluorescent microscopy. Western blot analysis confirmed the presence and expression levels of proteins. Additionally, we utilized an insoluble protein purification assay to validate the observed aggregates. Notably, our experiments revealed surprising findings, such as NDE1-inducing aggregation in mutant TRIOBP-1 and the co-aggregation of Flag-NDE1 and EGFP. These results shed light on the complex ways in which NDE1 can interact with other proteins.

This research unveiled intricate protein interactions, emphasizing the ongoing need for a deeper understanding of this disorder. By unravelling the links between protein aggregation and schizophrenia, studies like this pave the way

for more accurate diagnostics and innovative treatment approaches. These insights hold the promise of enhancing the quality of life for individuals with schizophrenia and driving further progress in this area.

KEY WORDS: Schizophrenia, TRIOBP-1, NDE1, protein aggregation, mental illness

Sažetak

Schizofrenija je kronična mentalna bolest koja utječe na ljude diljem svijeta i predstavlja značajan izazov u području mentalnog zdravlja. S obzirom na globalni porast njezine prevalencije, postaje sve važnije razumjeti njezine temeljne molekularne mehanizme. Složenost ove i drugih kroničnih mentalnih bolesti stvara znatne izazove u dijagnostici i liječenju, što ističe potrebu za inovativnim pristupima za razumijevanje njihove složene prirode. Nedavna otkrića, kao i fokus ovog rada, imaju za cilj staviti fokus na pojavu agregacije proteina u kontekstu schizofrenije, nudeći nove perspektive uz genetiku i čimbenike okoliša. Ovaj rad usredotočuje se na koagregaciju TRIOBP-1 i NDE1, od kojih oba igraju ključne uloge u staničnim procesima i neurobiologiji, te istražuje njihovu interakciju kako bi se razotkrili njihovi doprinosi tom poremećaju. Prethodne studije potvrđuju interakcije NDE1 s agregirajućim proteinima poput TRIOBP-1 i DISC1, ističući njegovu važnost u tom kontekstu.

Kako bismo dalje istražili ovu koagregaciju, koristili smo niz metodologija. Plazmide smo izrazili u stanicama neuroblastoma te smo njihove interakcije vizualizirali upotrebom imunofluorescentne mikroskopije. Western blot analiza potvrdila je prisutnost i razine izraženih proteina. Nadalje, koristili smo esej purifikacije netopivih proteina kako bismo potvrdili promatrane aggregate. Značajno je da su naši eksperimenti otkrili iznenađujuće rezultate, poput NDE1 koji potiče agregaciju mutiranog TRIOBP-1 i koagregaciju Flag-NDE1 i EGFP-a. Ti rezultati stavljaju fokus na kompleksne načine na koje NDE1 može interagirati s drugim proteinima.

Ovo istraživanje otkrilo je kompleksne interakcije proteina, naglašavajući stalnu potrebu za dubljim razumijevanjem ovog poremećaja. Razotkrivanjem veza između agregacije proteina i schizofrenije, istraživanja poput ovog otvaraju put za precizniju dijagnostiku i inovativne pristupe liječenju. Ovi uvidi

obećavaju poboljšanje kvalitete života osoba sa schizofrenijom i potiču daljnji napredak u ovom području.

KLJUČNE RIJEČI: Schizofenija, TRIOBP-1, NDE1, agregacija proteina, mentalne bolesti

Table of contents

1. Introduction	1
1.1. Chronic mental illness	1
1.2. Schizophrenia	2
1.2.1. Symptoms, diagnosis, and treatment.....	2
1.2.2. Physiological perspectives and potential research viewpoint.....	3
1.3. Proteinopathy	5
1.3.1. Proteins aggregating in chronic mental illness.....	7
1.4. TRIO and F-actin-Binding Protein 1.....	7
1.4.1. TRIOBP-1 in mental illness	8
1.4.2. TRIOBP-1 domain structure	10
1.5. Nuclear Distribution Factor E Homolog 1.....	11
1.5.1. NDE1 in mental illness	12
1.5.2. NDE1 domain structure.....	13
2. Aims of the thesis	15
3. Materials and methods	16
3.1. Materials	16
3.1.1. Plasmids and vectors.....	16
3.1.2. Antibodies and fluorescent markers	17
3.1.3. Size markers	17
3.2. Methods	18
3.2.1. Bacterial culture, transformation, and inoculation.....	18
3.2.2. Plasmid DNA purification	18
3.2.3. Micro-volume measurement of plasmid DNA.....	19
3.2.4. Agarose gel electrophoresis	19

3.2.5. Gateway cloning: LR clonase reaction	20
3.2.6. Cell culture.....	21
3.2.7. Transfection	22
3.2.8. Cell lysis	23
3.2.9. SDS-PAGE and Western blot.....	24
3.2.10. Immunocytochemistry and microscopy	25
3.2.11. Insoluble fraction purification	26
3.2.12. Treating cells with nocodazole.....	28
4. Results	29
4.1. Verifying protein size and expression by Western blot	30
4.2. Confirming previous results that TRIOBP-1 can co-aggregate with NDE1	32
4.3. Co-aggregation of TRIOBP-1 and NDE1 is not dependent on the plasmid vectors used.....	35
4.4. NDE1 is insoluble in the cell, suggesting it may aggregate	38
4.6. Testing protein insolubility after nocodazole treatment	41
4.5. NDE1 and NDEL1 behave similarly in HEK293T cells to SH-YS5Y cells	43
5. Discussion	46
5.1 Co-aggregation of TRIOBP-1 and NDE1	47
5.2 NDE1 as a potential aggregating protein.....	51
5.3. Future research directions	55
6. Conclusion	57
7. References.....	59
Appendix	65

1. Introduction

1.1. Chronic mental illness

Mental health refers to a state of well-being that encompasses emotional, psychological, and social aspects of an individual's life. Mental health affects how people think, feel, and act, and it plays a crucial role in determining how individuals handle stress, make choices, and relate to others. Various factors, such as genetic, biological, environmental, and psychosocial ones, can increase an individual's susceptibility to experiencing mental health issues. These factors involve genetic variations, brain chemistry, trauma, substance use, as well as a family history of mental health problems¹. Today, it is estimated that 1 in 8 individuals is living with a mental health condition².

Mental illnesses can vary in severity and duration, ranging from temporary conditions to chronic disorders. Chronic mental illness (CMI) refers to mental health conditions that are characterized by long-lasting symptoms and a persistent or recurring course over an extended period. Common mental illnesses include depression, anxiety disorders, bipolar disorder, schizophrenia, and eating disorders³.

Managing CMIs predominantly involves a combination of pharmacological treatments, such as mood stabilizers or antipsychotic medications, and psychosocial interventions, including psychotherapy, such as cognitive-behavioural therapy, and supportive services. The primary focus tends to be on managing and alleviating symptoms rather than addressing the underlying illness itself. Consequently, scientific research has increasingly focused on investigating these conditions' complex molecular mechanisms and biological foundations.

1.2. Schizophrenia

Schizophrenia is a global mental disorder that impacts approximately 24 million individuals worldwide, as reported by the World Health Organization⁴. Schizophrenia is a chronic and severe mental disorder that affects how a person thinks, feels, and behaves. The onset is commonly identified during the late teenage years or early adulthood, although it is known that the condition starts earlier and tends to manifest later in females⁵. It is a complex disorder that is believed to be caused by a combination of genetic, environmental, and brain chemistry factors.

1.2.1. Symptoms, diagnosis, and treatment

Schizophrenia is characterized by a wide range of symptoms that can be broadly categorized into three main groups: positive symptoms, negative symptoms, and cognitive symptoms. Positive symptoms involve an excess or distortion of normal thoughts, emotions, and behaviours. These include hallucinations (perceiving things that are not there), delusions (holding false beliefs), disorganized thinking and speech, and disorganized behaviour. Negative symptoms represent a loss or reduction of normal thoughts, emotions, and behaviours. They include flat affect (reduced emotional expression), social withdrawal, anhedonia (loss of pleasure), and avolition (lack of motivation). Cognitive symptoms affect cognitive processes and can impair functioning. These symptoms include impaired working memory, attention deficits, executive dysfunction, and difficulties in verbal and visual learning⁶.

Unfortunately, there are still some challenges surrounding chronic mental illnesses that have not been resolved. One of these is the diagnosis, which has remained unchanged for a long time; it is based solely on the symptoms that patients express and the ICD-10 (International Classification of Diseases). To

be diagnosed with schizophrenia, by the ICD-10 criteria, the patient must experience two or more of the previously mentioned symptoms over a significant portion of time during 1 month with the main ones being delusions, hallucinations, or disorganized speech⁷.

In the treatment of schizophrenia, a multifaceted approach is used, encompassing medication, psychosocial interventions, and supportive services. Firstly, antipsychotic medications play a crucial role in restoring neurotransmitter balance⁸. Moreover, psychosocial interventions are focused on enhancing social functioning and coping skills⁹. Additionally, Cognitive Behavioral Therapy (CBT) targets maladaptive thoughts and behaviors¹⁰. Furthermore, self-help and peer support groups provide valuable shared experiences and coping strategies¹¹. Additionally, integrated treatment approaches address the challenge of co-occurring substance use disorders¹². Lastly, individualized treatment plans, regular monitoring, and ongoing support are essential components of long-term care¹³.

1.2.2. Physiological perspectives and potential research viewpoint

Physiological perspectives offer valuable insights into the understanding of schizophrenia, shedding light on the biological underpinnings of the disorder. These perspectives explore various aspects, including brain structure abnormalities, neurotransmitter imbalances, genetic influences, epigenetic modifications, and immunological factors. By examining the physiological factors associated with schizophrenia, researchers aim to unravel the intricate mechanisms and provide a foundation for developing targeted interventions and treatments.

When examining the brains of individuals with schizophrenia, structural abnormalities have been consistently observed. Specifically, reductions in grey matter volume, particularly in the prefrontal cortex and hippocampus, have been identified¹⁴. Furthermore, disruptions in white matter connectivity,

which impair communication between different brain regions, have also been documented¹⁵ and associated with a higher probability of treatment resistance¹⁶.

Dysregulation of neurotransmitters plays a significant role in the pathophysiology of schizophrenia. Notably, the dopamine dysregulation hypothesis suggests an overactivity of dopamine signaling in specific brain areas, contributing to the positive symptoms of schizophrenia¹⁷. In addition, glutamate abnormalities, particularly related to N-methyl-D-aspartate (NMDA) receptor hypofunction, have been associated with the disorder¹⁸. Serotonin imbalances, a potential target of second-generation antipsychotics, have also been linked to the cognitive and emotional dysfunctions seen in schizophrenia¹⁹.

Moreover, in recent years, growing evidence suggests an association between immune system dysregulation and schizophrenia. Abnormalities in the immune system, such as elevated levels of pro-inflammatory cytokines, the presence of autoantibodies, and maternal immune activation during pregnancy, have been linked to an increased risk of developing schizophrenia²⁰⁻²².

Genetic factors have long been recognized as key contributors to the development of schizophrenia. Twin and heritability studies have provided strong evidence confirming the significant influence of genetics in the development of schizophrenia. These family and twin studies consistently demonstrate higher concordance rates among monozygotic twins compared to dizygotic twins, suggesting that approximately 80% of the risk for schizophrenia can be attributed to genetic factors²³. Furthermore, genome-wide association studies have identified multiple genetic loci associated with schizophrenia, implicating various genes and pathways in its etiology²⁴.

Epigenetic modifications, which regulate gene expression without altering the DNA sequence, have emerged as an area of interest in schizophrenia research. Alterations in DNA methylation patterns and histone modifications have been reported in individuals with the disorder, potentially influencing gene expression and brain development²⁵. These epigenetic changes shed light on the interplay between genetic and environmental factors in the manifestation of schizophrenia.

Due to the complex nature of schizophrenia's pathophysiology and the multitude of genetic variants involved, our understanding of the condition's pathological mechanism and its strong genetic basis remains limited²⁴. Identifying specific protein targets for diagnosis and therapy is challenging due to this complexity. As a result, researchers have explored proteinopathy as a potential non-genetic physiological aspect of schizophrenia, adopting a complementary approach²⁶.

1.3. Proteinopathy

Proteostasis (protein homeostasis) refers to the intricate network of cellular mechanisms that ensure proper protein synthesis, folding, and degradation, maintaining the balance and functionality of proteins. Protein aggregation, often referred to as proteinopathy, is a complex phenomenon characterized by the disruption in proteostasis and accumulation of misfolded or improperly folded proteins which the cell failed to degrade by the proteasome or by autophagy (Fig 1)^{26,27}. This process leads to the formation of insoluble complexes or aggregates that can have significant implications for cellular function and overall health. Aggregated proteins can disrupt normal cellular processes, interfere with protein-protein interactions, and compromise the structural integrity of organelles. This phenomenon is not limited to a particular cell type or tissue; rather, it occurs across various biological

contexts and is most commonly associated with neurodegenerative disorders, however it has also been implicated in metabolic diseases, and certain types of cancer²⁸. The study of protein aggregation is essential for understanding the underlying mechanisms of these conditions and for developing targeted therapeutic strategies aimed at preventing or mitigating the harmful effects of misfolded protein aggregates.

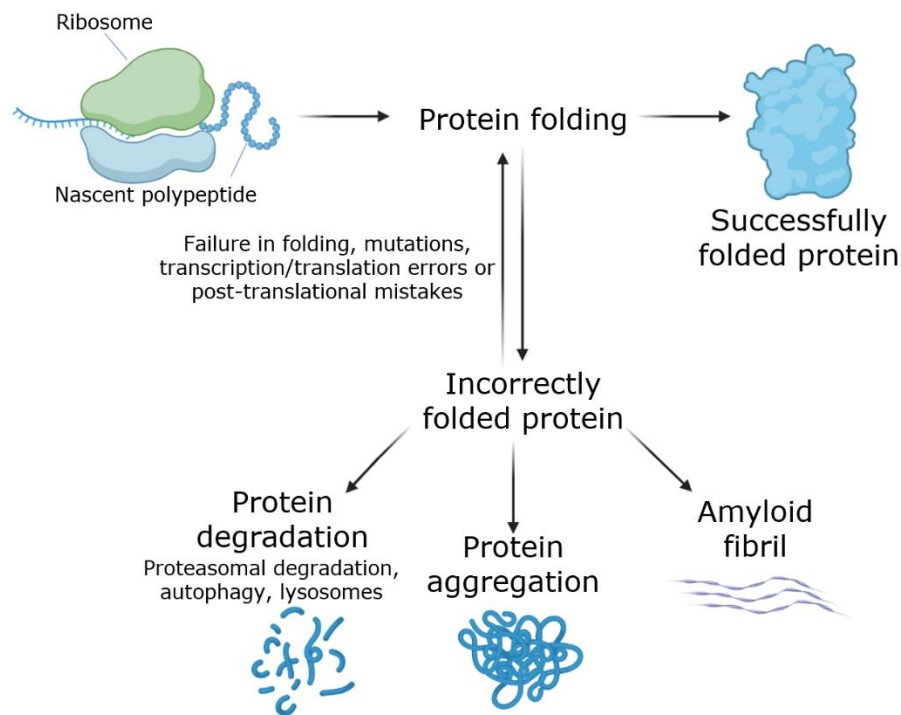


Figure 1: Schematic representation of misfolded protein fate. Proteins are synthesized with the help of protein folding machinery to achieve their functional form. However, errors in the folding process can lead to misfolding or protein aggregation. During protein synthesis, proteins go through a series of intermediate states to attain their fully functional, three-dimensional structure. If proteotoxic stresses or imbalanced conditions disrupt these processes, proteins can be misfolded. Misfolded proteins can either be refolded to their native state or degraded by cellular proteolysis mechanisms. However, if these mechanisms fail, misfolded proteins can accumulate and form amorphous aggregates or form amyloid fibrils. Made in BioRender.

1.3.1. Proteins aggregating in chronic mental illness

As the correlation between excessive expression and misfolding of proteins in a broad spectrum of neurodegenerative disorders has come to light²⁹, a recent approach in the field has shifted its focus toward identifying similar occurrences among patients with CMIs. In the context of conditions like schizophrenia, protein aggregation has gained significant attention, revealing potential connections to the disorder's neurobiology^{26,30}. The complex interplay of genetic, environmental, and neurobiological factors characterizing schizophrenia has prompted recent research to emphasize abnormal protein aggregation as a potential contributing factor. Specific proteins such as DISC1, dysbindin-1, CRMP1, TRIOBP-1, and NPAS3 have been linked to schizophrenia's pathology, exhibiting aggregated forms in affected individuals²⁶. These aggregated proteins have the potential to disrupt crucial cellular processes, impacting synaptic communication, neuronal connectivity, and overall brain function. While the exact mechanisms by which protein aggregation contributes to the development of schizophrenia are still being studied, investigating the role of protein aggregation in schizophrenia could offer valuable insights into the underlying mechanisms of the disorder, potentially leading to the development of novel treatment approaches that target abnormal protein interactions and restore proper neuronal function.

1.4. TRIO and F-actin-Binding Protein 1

Trio and F-actin-Binding Protein 1 (TRIOBP-1 or Tara) possess enigmatic roles in the brain that remain to be fully clarified. However, its critical involvement in actin polymerization is well-established, by directly binding to polymerized F-actin fibers, it regulates actin cytoskeletal organization and, in that way, impacts cell cycle regulation and migration. It is encoded by the multifaceted *TRIOBP* gene, which generates numerous splice variants including *TRIOBP-1* and *TRIOBP-4*³⁰. *TRIOBP-1*, arising from the gene's 3' end, is expressed across

various cell types and contributes to actin fiber formation³¹. Conversely, *TRIOBP-4*, emerging from the 5' end, finds expression primarily in the inner ear and retina, linked to ear rootlet function and deafness-causing mutations^{32,33}. Despite sharing a crucial role in actin polymerization, *TRIOBP-1* and *TRIOBP-4* lack common exons. As *TRIOBP-4*'s expression is confined to the ears and eyes, it makes its connection to mental disorders improbable. In contrast, the extensive isoform *TRIOBP-5*, exceeding 200 kDa, incorporates exons from both *TRIOBP-1* and *TRIOBP-4*, yet lacks in-depth characterization^{26,30}. While the specific brain functions of *TRIOBP-1* beyond actin polymerization remain hazy, studies confirm its involvement in neurite outgrowth, cell migration, proliferation, and chromosome segregation during mitosis. It is known to interact with various proteins and cellular structures, contributing to its diverse functions within the cell.

1.4.1. *TRIOBP-1* in mental illness

Recent research has revealed that ubiquitously expressed *TRIOBP-1* exhibits a propensity to form insoluble aggregates in the context of CMIs, notably schizophrenia. *TRIOBP-1* was identified in insoluble aggregates obtained from post-mortem brain tissue samples of schizophrenia patients³⁰. This experiment involved immunization of mice with insoluble proteins extracted from brain samples of schizophrenia patients. Prior to this discovery, the identification of monoclonal antibodies that selectively recognize unique epitopes was a crucial step. Notably, one such monoclonal antibody, 6H11, exhibited reactivity specifically towards the brain aggregomes of schizophrenia patients. While this antibody initially recognized an epitope on CRMP1, it also demonstrated an affinity for an additional protein³⁴. Subsequent investigations highlighted *TRIOBP-1* as the primary target of this monoclonal antibody, suggesting a potential link between *TRIOBP-1* and schizophrenia. Although the gene encoding *TRIOBP-1* is not suggested to be a direct genetic risk factor

due to its fundamental role in cell maintenance and proliferation, it was notable that TRIOBP-1 exhibited aggregation tendencies in both in vitro mammalian cell cultures and rat primary neurons, particularly after differentiation³⁰. The year 2017 marked a significant breakthrough, as Bradshaw *et al.* identified TRIOBP-1's central domain as the source of its aggregation propensity, pinpointing an essential 25-amino acid 'linker' region³⁵. Further studies, by Zaharija *et al.*, have refined this region even further to a sequence of just 8 amino acids. TRIOBP-1 constructs revealed that a concise 8-amino acid stretch (333-340) and an optional 59 amino acids at the extreme N-terminus could independently induce aggregation. As a result, the longer isoform of TRIOBP-1, spanning 597 amino acids and often referred to as "Tara" or "TAP68," demonstrated a reduced potential for aggregate formation³⁶.

TRIOBP-1's interactions with other proteins involved in neuronal development, such as NDE1 and NDEL1³⁷, indicate its involvement in processes like neuronal migration and cytoskeletal organization. Disruptions in these processes have been linked to the pathophysiology of schizophrenia, which involves abnormal connectivity and organization of brain circuits. While not directly implicated genetically, TRIOBP-1's aggregation tendencies in schizophrenia patients' brain aggregomes suggest a role in the complex molecular mechanisms underlying mental illnesses, necessitating further exploration of its contributions to the onset and progression of such disorders.

1.4.2. TRIOBP-1 domain structure

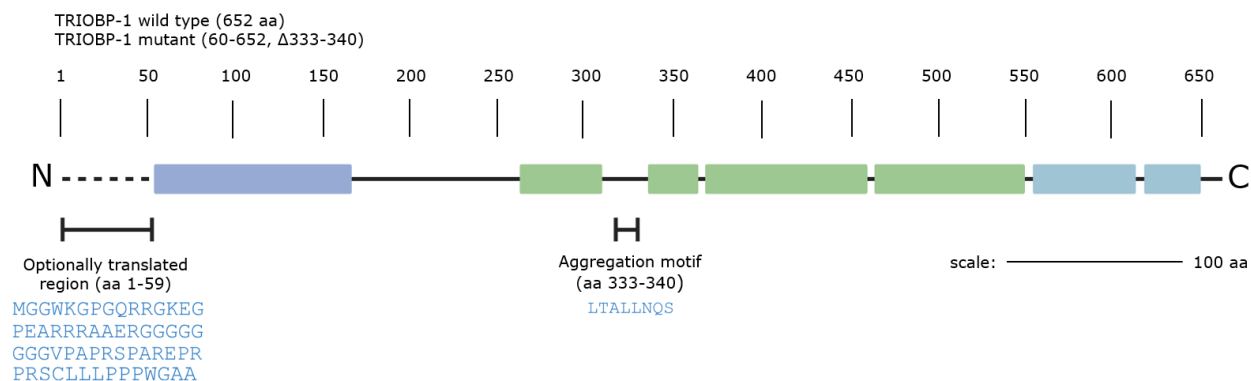


Figure 2: The predicted domain structure of TRIOBP-1. The predicted localization of the PH domain is represented by the purple rectangle. Coiled coils, here represented as green and blue rectangles, are coloured based on their predicted inclusion in the central CC domain (green) or C-terminal CC domain (blue). The amino acid sequences 1-59 and 333-340, included in the picture, were found to be responsible for the aggregation of TRIOBP-1. Adapted from Bradshaw et al. 2017 and Zaharija et al. 2022^{35,36}.

To gain a more comprehensive understanding of TRIOBP-1's specific functions and factors that trigger its aggregation, delving into its domain structure becomes imperative. Bradshaw *et al.* postulated that TRIOBP-1 encompasses three distinct domains within its 652 amino acid sequence. Within these, is the N-terminal pleckstrin homology (PH) domain (aa 60-189), characterized by a distinctive folded structure, with a significant β -sheet composition ($\sim 50\%$). This PH domain, when expressed as a recombinant protein, takes on a soluble, stable dimeric form. The other two domains reside in the protein's C-terminal portion: the central domain (aa 281-555) and the C-terminal domain (aa 556-652), both adapting α -helical structures, likely in the configuration of coiled-coil domains (CC). Both the PH and central domains are associated with the promotion of neurite growth. When expressed independently, the C-terminal domain forms a stable, monomeric protein. The researchers hypothesized that the C-terminal half encompasses six coiled-coil regions, designated as CC1 through CC6. This arrangement entails the central domain encompassing CC1-CC3/CC4, while the C-terminal domain comprises

CC5-CC6. The central domain plays a pivotal role in TRIOBP-1's oligomerization and in preventing F-actin depolymerization. Positioned before the PH domain is an additional N-terminal region spanning 59 amino acids (amino acids 1-59), characterized by an abundance of prolines and seven positively charged residues. This optional N-terminal region, when expressed in neuroblastoma cells, localizes within both the cytoplasm and nucleus and it was discovered that it contributes to aggregation. Between the initial two coiled-coil regions of the central domain, CC1 and CC2, lies an essential 25-amino acid stretch, commonly referred to as the "linker" region (amino acids 324-349), which is responsible for the protein's aggregation properties³⁵. The region responsible for aggregation, contained within the "linker" region, was later identified to be 8 amino acids long (aa 330-340), discovering a non-aggregating TRIOBP-1 mutant (60-652, Δ 333-340). A most recent study has revealed that TRIOBP-1's aggregation propensity involves two mechanisms based on its extreme N-terminus and the loop between two coiled-coils in the central region, with the longer 652 amino acid form of TRIOBP-1 exhibiting two aggregation pathways. Smaller TRIOBP species detected in brain samples and cell systems are thought to possess only the central aggregation critical region³⁶.

1.5. Nuclear Distribution Factor E Homolog 1

Nuclear Distribution Factor E Homolog 1 (NDE1, NudE) and NDEL1 (NudE-like-1, Nudel) are closely related proteins that play significant roles in various cellular processes, such as the organization of the microtubule cytoskeleton and neurodevelopment³⁸.

One of NDE1's key interactions is with tubulin, a protein that makes up microtubules, which are essential components of the cytoskeleton and play crucial roles in cell division, intracellular transport, and maintaining cell shape.

Microtubules are highly dynamic structures that can undergo polymerization (growth) and depolymerization (shrinkage), allowing cells to rapidly rearrange their cytoskeleton to perform various functions. In neurodevelopment, NDE1's interaction with tubulin is particularly important for processes like neuronal migration. Proper neuronal migration is essential for the formation of functional brain circuits³⁹. Located in the centrosome, NDE1 and NDEL1 are part of a multiprotein complex, which interacts with cytoplasmic dynein, a molecular motor protein involved in intracellular transport along microtubules³⁹. Dysfunction in processes like microtubule dynamics, cytoskeleton organization, and centrosome function, with which both are known to interact, can lead to abnormal brain development and potentially contribute to the development of neuropsychiatric disorders. Mutations or dysregulation of NDE1 and NDEL1 have been associated with several neurodevelopmental and psychiatric disorders ^{40,41}.

1.5.1. NDE1 in mental illness

NDE1 has emerged as a significant player in the context of mental illness, particularly in conditions like schizophrenia, due to its potential involvement in the disease's underlying mechanisms. Disruptions in fundamental processes like neuronal migration, synaptic connectivity, and overall brain structure are thought to contribute to the pathogenesis of mental illnesses, including schizophrenia. Moreover, NDE1's interactions with other proteins, such as LIS1, TRIOBP-1 and DISC1, have been linked to protein aggregation, a phenomenon implicated in various neurodegenerative disorders^{37,39,41}. The interplay between NDE1 and these proteins suggests a complex network of molecular interactions that could influence the development and progression of the disorder. The involvement of NDE1 in multiple aspects of neuronal development and its connections to protein aggregation is thought to contribute to the manifestation of schizophrenia symptoms, highlighting its

potential as a key player in the complexity of the disease. Given NDE1's involvement in tubulin interaction and microtubule regulation, it is plausible that abnormalities in these interactions could also contribute to the neurobiological underpinnings of schizophrenia. However, the exact mechanisms through which NDE1's interactions with tubulin may contribute to schizophrenia are complex and are an area of ongoing research.

1.5.2. NDE1 domain structure

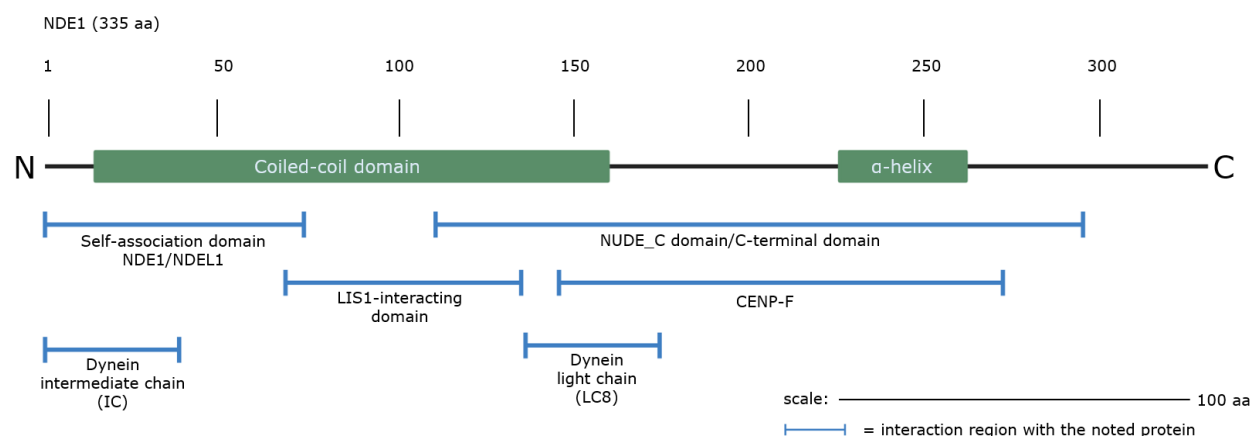


Figure 3: The predicted domain structure of NDE1 and its interaction regions. The predicted domain structure of human NDE1 consists of three main domains: a self-association domain, a LIS1 interaction domain, and a NUDE_C domain at its C terminus. The self-association domain and LIS1 interaction domain share the first five amino acids. The protein is 335 amino acids long and is primarily composed of coiled coils and alpha helices. NDE1 interacts with various binding partners, and these interactions are indicated by blue lines and labels. Adapted from Bradshaw et al. 2013 and Soto-Perez et al. 2020^{42,43}.

The main isoform of NDE1 is a protein comprised of 335 amino acids and primarily composed of alpha-helices whose structure consists of distinct domains that contribute to its functions within the cell⁴². The predicted domain structure of human NDE1 consists of three main domains: a self-association domain, a LIS1 interaction domain, and a NUDE_C domain at its C terminus. The self-association domain and LIS1 interaction domain share the first five amino acids. One of the prominent domains in NDE1 is the LisH domain, which

is involved in protein-protein interactions. This domain is critical for NDE1's ability to interact with other proteins and form complexes that are essential for various cellular processes, including the already mentioned neuronal migration and organization. Another important domain in NDE1 is the coiled-coil domain. This domain is known for its role in mediating protein-protein interactions and forming stable protein complexes. In NDE1, the coiled-coil domain contributes to its interactions with other proteins involved in neurodevelopment and cellular organization. The C-terminal region of NDE1 contains a nuclear localization signal (NLS), which directs the protein to the cell nucleus. This region is important for regulating NDE1's subcellular localization and function within the nucleus. Within the C-terminal domain is the CENP-F binding site, which binds a nuclear matrix component, CENP-F, which localizes to kinetochores during mitosis and is rapidly degraded afterwards. Dynein subunits bind to different locations on NDE1, with the interaction site of dynein intermediate chain (IC) located in the self-association domain, whereas dynein light chain (LC8) interacts with the C-terminal domain⁴³.

The structure of NDE1, with its LisH domain, coiled-coil domain, and nuclear localization signal, enables the protein to participate in a range of critical cellular processes, and potentially influence interactions with other proteins implicated in neurodevelopmental disorders such as schizophrenia. The specific interactions and functions of NDE1's domains continue to be a subject of investigation, as researchers seek to uncover its precise contributions to neuronal development and the potential implications for various neurological and psychiatric conditions.

2. Aims of the thesis

Recent research into CMIs, including schizophrenia, bipolar disorder, and major depressive disorder, has identified proteins like TRIOBP-1, CRMP1, NPAS3, DISC1, and Dysbindin-1, which aggregate in patients. The nature of these protein aggregates and their potential co-aggregation with interacting partners in functional form remains unclear. Protein aggregation has been linked with chronic brain disorders since its discovery in Alzheimer's disease and has emerged as an important theme in the study of schizophrenia. TRIOBP-1's association with schizophrenia raises questions about its potential to induce co-aggregation with partners like NDE1, impacting brain function. The importance of understanding the biological basis of CMIs due to limited research is evident.

We will therefore test the hypothesis of TRIOBP-1's ability to recruit NDE1 to aggregate when co-expressed. In addition, NDE1, which is known to be involved in CMIs, exhibits uniform expression when expressed in SH-SY5Y cells, but when co-expressed with TRIOBP-1 leads to the formation of aggregates³⁷, highlighting its potential role as a co-aggregation partner in CMIs and schizophrenia. The interaction between NDE1 and TRIOBP-1 in their functional forms is not unexpected, given their roles in neurodevelopment and oligodendrocyte differentiation.

Based on previous TRIOBP-1 and NDE1 research, in this thesis, we aimed to:

- 1) Verify the co-aggregation of wild-type TRIOBP-1 and NDE1, including using alternative vectors.
- 2) Investigate whether co-expression of NDE1 and mutated non-aggregating TRIOBP-1 leads to aggregation.
- 3) Determine if the co-aggregation of NDE1 and TRIOBP-1 is related to the role of NDE1 as a tubulin-binding protein.

3. Materials and methods

3.1. Materials

3.1.1. Plasmids and vectors

Table 1: List of expression and entry vectors

Protein encoded	Vector	Antibiotic resistance	Publication	Source
NDE1	pdcdNA-FlagMyc	Ampicillin	Unpublished	N. Bradshaw, Düsseldorf
NDE1	pDONR	Zeocin	Unpublished	N. Bradshaw, Düsseldorf
NDE1	pDEST-CMV-N-EGFP	Ampicillin	Unpublished	Generated as part of this thesis
TRIOBP-1	pdcdNA-Flag	Ampicillin	Bradshaw et al. (2017) ³⁵	N. Bradshaw & C. Korth, Düsseldorf
TRIOBP-1	pDEST-CMV-N-EGFP	Ampicillin	Samardžija et al. (2023) ⁴⁴	M. Juković & N. Bradshaw, Rijeka
TRIOBP-1 (60-652, Δ333-340)	pdcdNA-Flag	Ampicillin	Zaharija et al. (2022) ³⁶	B. Zaharija & N. Bradshaw, Rijeka
Control	pDEST-CMV-N-EGFP	Ampicillin	Samardžija et al. (2023) ⁴⁴	B. Zaharija & N. Bradshaw, Rijeka
Empty	pDEST-CMV-N-EGFP	Ampicillin/ Chloramphenicol	Agrotis et al. (2019) ⁴⁵	R. Ketteler, University College London, UK

3.1.2. Antibodies and fluorescent markers

Table 2: List of primary and secondary antibodies, as well as nuclear and cytoskeletal stains used in Western blot and cell staining (immunocytochemistry)

Name	Supplier	Concentration	Dilution
Anti-Flag M2 – Monoclonal (mouse)	Sigma	1 mg/mL	1:2000
Anti-GFP – Monoclonal (mouse)	Sigma	1 mg/mL	1:2000
Peroxidase Conjugated Affinity Purified Goat anti-Mouse IgG	Thermo Fisher Scientific	1 mg/mL	1:2000
Alexa Fluor 555 Goat anti-Mouse IgG	Thermo Fisher Scientific	2 mg/mL	1:1000
DAPI	Sigma	1 mg/mL	1:500

3.1.3. Size markers

My-Budget 1kb DNA Ladder (200 mg/mL)- Bio Budget Technologies GmbH

The marker consists of 13 blunt-ended fragments in the range from 250 base pairs (bp) to 10 kilobase pairs (kbp). It is used for gel electrophoresis.

My-Budget 100 bp + 1.5 kb DNA Ladder – Bio Budget Technologies GmbH

The marker consists of 10 blunt-ended fragments in the range from 100 bp to 1000 bp, with an additional fragment at 1500 bp. It is used for gel electrophoresis.

My-Budget Prestained Protein Ladder 10-180 kDa (0.2-0.4 µg/µL) - Bio Budget Technologies GmbH

The marker consists of proteins in the size range between 10 kDa - 180 kDa with an additional fragment at 1500 bp and is used for Western Blot transfers performed in Tris-Glycine buffer.

3.2. Methods

3.2.1. Bacterial culture, transformation, and inoculation

The bacterial transformation was conducted using NEB5 α competent bacterial cells to generate a substantial quantity of the desired DNA copies. This approach facilitated efficient replication and amplification of the target DNA on a large scale. As a first step, 1 μ L of plasmid construct was added to a sterile 1.5 mL Eppendorf tube containing 50 μ L of freshly thawed NEB5 α cells and incubated on ice for 30 minutes. The incubation was followed by heat shock transformation, at 42°C for 30 seconds, and a 5-minute recovery on ice. Following the recovery period on ice, the suspension was then inoculated on LB agar (see appendix for buffer/media/solutions recipes) plates containing antibiotic ampicillin (1 μ L/mL) and grown overnight with plates upside-down in the incubator at 37°C. After overnight incubation, a single colony was picked and, again, grown overnight in 3 mL of LB media (see appendix) with antibiotic ampicillin in a shaking incubator (37°C/250 rpm). The next day, the liquid bacterial culture was pelleted by centrifugation at 3700 rpm for 15 minutes and plasmid DNA was purified and isolated as per the protocol described below.

3.2.2. Plasmid DNA purification

Plasmid DNA was isolated using the QIAprep Spin Miniprep Kit in accordance with the manufacturer's instructions. The bacterial pellet from the centrifuged liquid culture was resuspended in buffer P1 and lysed with buffer P2. A 5-minute neutralization with buffer N3 was followed by centrifugation of the suspension in a table-top microcentrifuge at 13000 rpm for 10 minutes. The supernatant obtained was then applied onto the QIAprep 2.0 spin column and

centrifuged for a duration of 30-60 seconds. The supernatant was removed following each subsequent centrifugation and discarded. Next, the QIAprep 2.0 spin column was washed using buffer PB and centrifuged once again. Following this, buffer PE was added, and another centrifugation step was performed. To ensure the complete removal of any residual washing buffer, an additional 1-minute centrifugation of the QIAprep 2.0 spin column was carried out. Finally, DNA was eluted from the column using buffer EB by briefly incubating at room temperature (RT) and centrifuging for 1 minute. The resulting samples were stored in the freezer at -20°C.

3.2.3. Micro-volume measurement of plasmid DNA

The concentration of samples obtained from bacterial culture growth and plasmid DNA purification was determined using a BioDrop μ LITE spectrophotometer. The absorbance wavelength was set at 260 nm, and elution buffer EB was used as a blank reference. A volume of 1 μ L from each sample was analyzed, and the measured concentrations were reported in ng/ μ L.

3.2.4. Agarose gel electrophoresis

The confirmation of purified plasmid DNA samples was achieved through agarose gel electrophoresis, a technique used to separate DNA molecules based on their size. Agarose gel was prepared by mixing agarose, 1x TAE buffer (see appendix), and Gel Green dye, which was then heated in the microwave until complete dissolution. Once the gel solidified, it was placed in an electrophoresis tank filled with 1x TAE buffer.

For each sample, 10 µL of a solution containing distilled water, DNA loading buffer (see appendix), and purified plasmid DNA was loaded onto the gel. Additionally, 3 µL of a marker consisting of a DNA ladder and DNA loading buffer was included. The electrophoresis process was conducted at 140 V for a duration of 15-20 minutes. The resulting gel was visualized using a BioRad Chemi-Doc MP Imaging System.

3.2.5. Gateway cloning: LR clonase reaction

The full-length human NDE1 was transferred into the destination vector pDEST-CMV-N-EGFP using the Gateway cloning system. This was accomplished using the LR clonase recombination reaction.

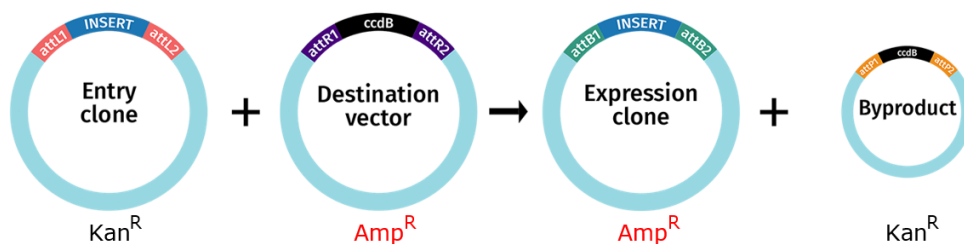


Figure 4: Gateway LR Clonase recombination reaction scheme. In this reaction, the entry vector typically includes attachment sites L (attL1/attL2), whereas the destination vector contains the complementary attachment sites R (attR1/attR2), an antibiotic resistance gene (AMP), and a death cassette. Adapted from www.snapgene.com.

LR recombination is catalysed by the addition of the LR clonase enzyme mix, allowing the DNA fragment to be transferred from the entry clone to the destination vector. This results in the formation of a final construct in the destination vector, i.e., NDE1 with an EGFP fusion protein at its N-terminus. The recombination reaction was performed by adding pDONR/Zeo-NDE1 as an entry vector, pDEST-CMV-N-EGFP as a destination vector, TE buffer (see appendix) and Gateway LR clonase enzyme mix to a sterile 1.5 mL Eppendorf tube as specified in the Table 3 below.

Table 3: LR clonase reaction

	Component	Amount
Entry vector	pDONR/Zeo-NDE1	50-150 ng
Destination vector	pDEST-CMV-N-EGFP	150 ng
	TE buffer [pH 8.5]	Up to 9 μ L
	LR clonase enzyme mix	1 μ L
	Proteinase K (after 1h)	1 μ L

The reaction mixture was then incubated at room temperature (RT, 25°C) for 1 hour. After the incubation, the reaction was terminated with the addition of Proteinase K followed by incubation in the shaking incubator at 37°C/250 rpm for 7 minutes. According to the previously described technique in section 3.2.1., 5 μ L of the sample was used to transform the NEB5 α bacteria, while the rest of the product was stored at -20°C. The clones that underwent recombination in such a way that they carried the ampicillin resistance gene in addition to the gene of interest are the ones that can grow on LB agar plates containing ampicillin. After that, the cultures were grown as usual, the DNA was isolated, examined on an agarose gel, and sent for sequencing.

3.2.6. Cell culture

Two cell lines, HEK293T and SH-SY5Y, were cultured individually. HEK293T cells, derived from human kidney cells, were chosen for their rapid growth rate and ease of transfection. On the other hand, SH-SY5Y cells, derived from human neuroblastoma cells, were selected as they provide a more suitable model for neuronal aspects. Different growth media were utilized for each cell line: DMEM (+/+) media (see appendix) for HEK293T and DMEM-F12 (+/+) (see appendix) for SH-SY5Y, with the inclusion of fetal calf serum (FCS) and

antibiotics (indicated as "+/+"). Both cell lines were cultivated in T25 flasks, with cells adhering to the bottom surface.

When the cells reached a confluency of 80-90%, they were subcultured into new T25 flasks or 6 or 12-well plates, depending on the specific experimental requirements. The subculturing process involved using preheated trypsin solution and the corresponding medium at 37°C. To ensure a sterile environment within the biological safety cabinet, all equipment and surfaces were sprayed with 70% ethanol before use.

To initiate the subculturing process, the old media was aspirated, and 1 mL of trypsin solution was added to the T25 flask containing cells ready for splitting. The flask was incubated at 37°C for approximately 5 minutes to allow trypsinization. After incubation, the flask was gently tapped to facilitate cell detachment. Following that, 4 mL of the appropriate medium was added to the old flask, and fresh media were prepared for the new flasks or plates.

In the case of SH-SY5Y cells intended for microscopic examination, glass coverslips were placed in the wells of the 12-well plates before adding media and cells. The cells from the old flask were then split into the new flask or plates based on the desired dilution, which depended on the confluency of cells in the old flask. For HEK293T cells intended for lysis and Western blotting, they were split into 6-well plates. On the other hand, SH-SY5Y cells were split into 12-well plates with glass coverslips for immunocytochemistry and microscopy purposes. All the flasks and plates were maintained in a Nüve CO₂ incubator at 37°C with a 5% CO₂ atmosphere.

3.2.7. Transfection

After cell passaging, the subsequent step involves transfection, a process in which DNA plasmids of interest are introduced into mammalian cells. For the

transfection procedure, HEK293T cells were transfected using Metafectene, while SH-SY5Y cells were transfected using Metafectene Pro. As previously mentioned, each cell line requires different media, namely DMEM/HEK293T and DMEM-F12/SH-SY5Y, without the inclusion of FCS or antibiotics (indicated as "-/-").

To prepare for transfection, two solutions were created. The DNA solution consisted of 100 µL/300 µL of "-/-" media (depending on the plate size of 6 or 12 wells) and an appropriate amount of plasmid DNA based on measured concentrations. The Metafectene/Metafectene Pro solution contained 2 µL of Metafectene or 6 µL of Metafectene Pro, along with 100 µL/300 µL of "-/-" media. After a 5-minute incubation at RT, the two solutions were mixed and incubated again for 20 minutes at RT.

Meanwhile, the wells were prepared by removing the regular "+/+" media (containing serum and antibiotics) and washing them with 0.5 mL/1.5 mL of corresponding "-/-" media. The media was then aspirated, and 300 µL/900 µL of fresh "-/-" media was added to the wells. Afterwards, the solution containing the DNA and transfection reagent was added to the wells, and the plates were incubated in a 37°C incubator for 6 hours.

After the 6-hour incubation period, the "-/-" media was replaced with fresh "+/+" media, and the plates were left to incubate overnight. Following transfection, HEK293T cells were lysed, and the resulting cell lysates were used for Western blot analysis. On the other hand, SH-SY5Y cells were utilized for immunocytochemistry and cellular imaging analysis.

3.2.8. Cell lysis

Following the overnight incubation period after transfection, the media was aspirated from the HEK293T cells, and the cells were washed twice with

phosphate-buffered saline (PBS). The PBS was then removed, and cell lysis buffer (see appendix) was introduced and allowed to sit for approximately 5 minutes. To the cell lysis buffer, DNaseI (1 μ L per mL of buffer) and protease inhibitor cocktail (at a final concentration of 1x) were added immediately prior to use. Using the buffer, the bottom of the wells was gently pipetted to ensure the removal of any remaining cells, and the solution was then transferred to 1.5 mL Eppendorf tubes. The solutions were incubated on ice for 1 hour with periodic vortexing. Following the incubation, the samples were either stored at -20 °C or prepared for Western blot analysis.

3.2.9. SDS-PAGE and Western blot

SDS-PAGE (sodium dodecyl sulfate-polyacrylamide gel electrophoresis) is a technique utilized to separate proteins based on their molecular weight. For SDS-PAGE, 8% and 10% acrylamide gels were prepared by manually casting them using the Mini-PROTEAN Tetra Handcast Systems from Bio-Rad (see appendix for recipe tables). The acrylamide stacking gel, with a lower polyacrylamide concentration, was placed on top of the more concentrated running gel. This stacking gel helps create an ionic gradient to concentrate the proteins into a single band. As the proteins enter the running gel with smaller pores, they separate according to their molecular weight.

After setting the stacking gel, lysates for Western blot analysis were thawed, and samples were prepared by adding Protein Loading Buffer (see appendix) and 1M DTT to the lysates. The solution was then denatured by heating at 95°C for 5 minutes. Following denaturation, the prepared samples, along with a Prestained Protein Ladder marker, were loaded onto the gel. SDS-PAGE was conducted for 50 minutes at 180V using SDS-PAGE Running Buffer (see appendix). The proteins from the gel were then transferred onto a polyvinylidene difluoride membrane (Macherey-Nagel, 0.20 μ m pore) using

the Trans-Blot Turbo Transfer System from Bio-Rad which ran at 0.5 A for 30 minutes.

Following the transfer, the membranes underwent several washing steps with water, Ponceau S (see appendix) staining solution, and PBS-Tween (PBS-T, see appendix) to visualize the total protein and remove any residual staining. The membranes were then blocked overnight at 4°C in PBS-T with 5% dry milk. Following the overnight blocking, they were incubated with primary antibodies diluted in PBS-T solution for 2-4 hours at RT on a shaker. After the primary antibody incubation, the membranes were incubated with secondary antibodies diluted in PBS-T for 1 hour at RT. Between each antibody incubation, the membranes were washed three times with PBS-T over a period of 30 minutes. To detect protein bands, Pierce ECL Western Blotting Substrate from Thermo Fisher was used, and chemiluminescent images were captured using the ChemiDoc MP Imaging System from Bio-Rad.

3.2.10. Immunocytochemistry and microscopy

Following transfection and an overnight incubation period, the SH-SY5Y cell line was utilized for immunocytochemistry and microscopy experiments. The DMEM-F12 (+/+) media was removed, and the transfected SH-SY5Y cells growing on glass coverslips were gently rinsed with 0.5 mL of PBS (see appendix) per well. After the gentle wash, the cells were fixed with Fixation buffer (see appendix) for 15 minutes, followed by permeabilization using Permeabilization buffer (see appendix) for an additional 10 minutes. After three washes with PBS, the cells were blocked with 10% goat serum in PBS for a minimum of 30 minutes (up to 1 hour). Following the blocking step, the blocking media was discarded, and a mixture of PBS containing the primary antibody and goat serum was added. The cells were incubated with the primary antibody, Anti-Flag for Flag-tagged proteins (this was not necessary

for the GFP fusion proteins, which, when visualized under a microscope, exhibit intrinsic fluorescence), which was diluted in 10% goat serum/PBS, for a duration of 1-3 hours. Following another round of three PBS washes conducted over 15 minutes, the cells were incubated in the dark with the secondary antibody, Goat anti-Mouse 555, along with DAPI, both of which were diluted in 10% goat serum/PBS, for 1 hour. The cells were covered with a wet paper towel during this incubation to maintain humidity. After the incubation, the secondary antibody solution was removed, and the cells were washed three times with PBS over 15 minutes. The entire procedure was carried out at RT. Finally, the glass coverslips were mounted onto slides using a Mounting medium and stored at 4°C until further analysis. The prepared coverslips were observed under an Olympus IX83 fluorescent microscope at 60x magnification. Images were captured using a Hamamatsu Orca R2 CCD camera and CellSens software, and further analysis was performed using the ImageJ program.

3.2.11. Insoluble fraction purification

The insoluble fractions from cell lysates were purified using an adapted protocol from previous research^{30,35}. The media in the wells was removed, and the cells were washed twice with PBS. Next, the cells were lysed by adding 200 µL of Lysis Buffer for Protein Extraction (see appendix) and allowing them to incubate for 5 minutes. The lysed cells were then collected into ultracentrifuge tubes (UC tubes) using a cell scraper, and 2.5 µL of Triton-X-100 (see appendix) was added per tube. Before centrifugation, 60 µL of the homogenate was collected as a sample for Western blot, which was prepared by mixing it with 60 µL of Protein loading buffer (see appendix) and 6 µL of DTT.

The samples in the UC tubes were spun at 20,000 x g for 20 minutes at 4°C (Thermo Scientific Sorvall MTX 150 Micro-Ultracentrifuge). The supernatant was carefully removed, and the pellet was subjected to another round of lysis by adding Lysis Buffer for Protein Extraction and Triton-X-100. After centrifugation at 20,000 x g for 20 minutes at 4°C, the supernatant was again removed, and the pellet was resuspended in 200 µL of buffer A1 (see appendix). The resuspended pellet was then subjected to centrifugation at 130,000 x g for 45 minutes at 4°C.

The process of resuspension and centrifugation in buffer A1 was repeated once more. After the final centrifugation, the supernatant was discarded, and the pellet was resuspended in 200 µL of buffer B1 (see appendix). The samples were then incubated either for 1 hour at 37°C or overnight at 4°C. Following the incubation, the samples were centrifuged at 130,000 x g for 45 minutes at 4°C. The supernatant was removed, and the pellet was resuspended again in 200 µL of buffer B1, this time without DNaseI. Another round of centrifugation at 130,000 x g for 45 minutes at 4°C followed.

The supernatant was once again removed, and the pellet was dissolved in 200 µL of buffer C1 (see appendix). An insulin syringe and a 0.4 mm needle were used to facilitate the dissolution. The samples were then incubated on ice for approximately 1 hour on a shaking tray. After the incubation, the samples were spun at 112,000 x g for 45 minutes at 4°C. The supernatant was discarded, and the previous step of resuspension in buffer C1 was repeated. Following another round of centrifugation at 112,000 x g for 45 minutes at 4°C, the supernatant was removed, leaving behind the final pellet.

Once the final insoluble pellet was obtained, it was dissolved in a loading buffer containing 20 µL of Protein loading buffer (see appendix) and 2 µL of DTT. The samples were then heated at 95°C for 5 minutes to denature the proteins and stored at -20°C for later use in Western blot. During the analysis phase, a

Western blot was performed by loading 10 μ L of each sample, along with 30 μ L of the homogenate obtained at the beginning of the protocol, into separate lanes of the gel and continued per the protocol described in 3.2.9.

3.2.12. Treating cells with nocodazole

In order to disrupt the microtubules within cells, a substance called nocodazole was employed prior to the purification of the insoluble fraction in transfected cells.

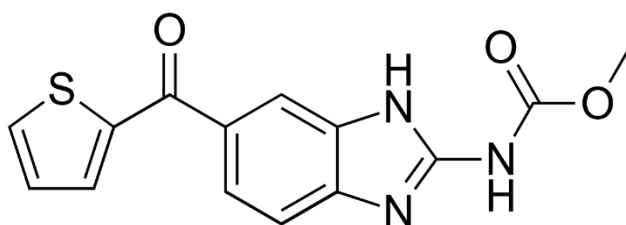


Figure 5: Nocodazole structure. Chemical formula: C₁₄H₁₁N₃O₃S, molecular weight: 301.3 g/mol. Taken from <https://en.wikipedia.org/>.

Nocodazole was prepared by diluting it in dimethyl sulfoxide (DMSO) to create a stock solution with a concentration of 1.25 mM. The working concentration of nocodazole used was 25 μ M. On the day of the insoluble fraction purification procedure, the culture media was removed from the wells containing HEK293T cells. One 6-well plate containing HEK293T cells was treated with nocodazole (10 μ L per 1 mL of DMEM (+/+) media) and incubated on ice for 45 minutes. Afterwards, it was placed in the refrigerator at 4°C for an additional 45 minutes. Two control plates were also prepared, each with 10 μ L of DMSO per 1 mL of DMEM (+/+). These control plates were likewise incubated on ice for 45 minutes, after which one plate was placed in the refrigerator at 4°C and the other in the incubator at 37°C, both for 45 minutes. Following the incubation period, the insoluble fraction was purified following the previously established protocol in section 3.2.11.

4. Results

As protein aggregation gains significant attention for its potential implications in the disorder's neurobiology, this thesis delves into the intersection of protein aggregation and chronic mental illnesses, particularly focusing on schizophrenia. The study of protein misassembly and aggregation has become a crucial focus in schizophrenia research, a field marked by its intricate interplay of genetic, environmental, and neurobiological factors^{26–28,30,44}. Building upon recent findings³⁷, this research investigates the co-aggregation dynamics of TRIOBP-1 and NDE1, both of which have been implicated in schizophrenia. By aiming to verify the co-aggregation of these proteins, explore the effects of mutated non-aggregating TRIOBP-1 on co-expression with NDE1, and discern the relationship between NDE1's role as a tubulin-binding protein and its co-aggregation with TRIOBP-1, this thesis seeks to contribute valuable insights into the underpinnings of protein aggregation in the context of schizophrenia.

Table 4: List of plasmids

Protein encoded	Vector	Antibiotic resistance	Publication	Source
NDE1	pdCDNA-FlagMyc	Ampicillin	Unpublished	N. Bradshaw, Düsseldorf
NDE1	pDEST-CMV-N-EGFP	Ampicillin	Unpublished	Generated as part of this thesis
TRIOBP-1	pdCDNA-Flag	Ampicillin	Bradshaw et al. (2017) ³⁵	N. Bradshaw & C. Korth, Düsseldorf
TRIOBP-1	pDEST-CMV-N-EGFP	Ampicillin	Samardžija et al. (2023) ⁴⁴	M. Juković & N. Bradshaw, Rijeka
TRIOBP-1 (60-652, Δ333-340)	pdCDNA-Flag	Ampicillin	Zaharija et al. (2022) ³⁶	B. Zaharija & N. Bradshaw, Rijeka
Control	pDEST-CMV-N-EGFP	Ampicillin	Samardžija et al. (2023) ⁴⁴	B. Zaharija & N. Bradshaw, Rijeka

4.1. Verifying protein size and expression by Western blot

Before investigating the aggregation and co-aggregation propensity of TRIOBP-1 and NDE1 we decided to confirm successful construct expression in mammalian cells. For that purpose, the human embryonic kidney (HEK293T) cell line was grown and transfected with constructs listed in Table 4.

Firstly, all the above-mentioned plasmid constructs were grown and isolated from NEB5α competent bacterial cells. These plasmids were then introduced into separate wells containing HEK293T cells, chosen for their facilitative transfection properties and suitability for Western blot analysis. Transfection was carried out using Metafectene as the transfection reagent. Post-transfection, the HEK293T cells underwent lysis, and the resulting samples were subjected to Western blot analysis. The visual representation of these blots (Figure 6) illustrates the expression levels of the specified constructs. Mock transfections included lysates obtained from cells not transfected with plasmid DNA. Notably, an anti-GFP antibody was employed as the primary antibody in Figure 6.A, while an anti-Flag antibody was used in Figure 6.B to bind with the expressed Flag tag within the protein. Detection was facilitated using Goat Anti-Mouse antibody as the secondary agent. The membranes were then visualized under ChemiDoc using the ECL visualization kit.

After running the samples on the blot and applying the staining procedure, we observed that all plasmid constructs displayed sizes on the blots that were consistent with the expected sizes (Figure 6). This outcome provided concrete evidence that the proteins were indeed present and expressed as intended in the samples we examined.

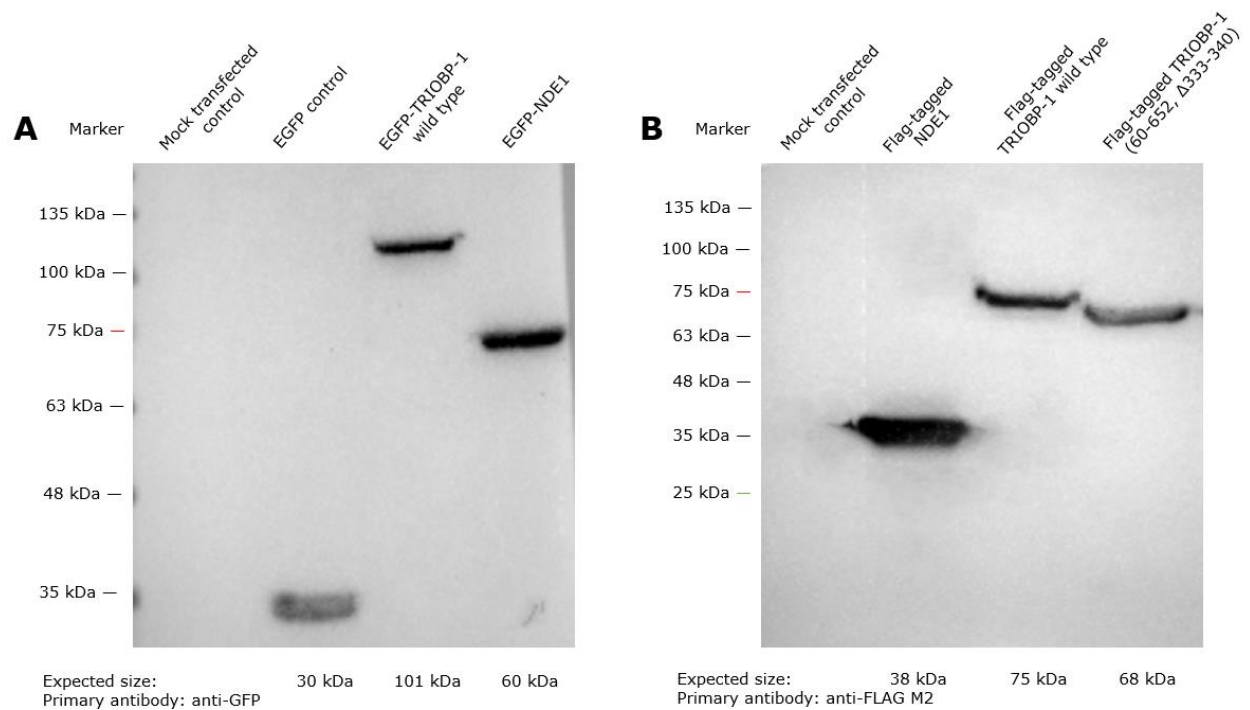


Figure 6: Western blot analysis for anti-GFP and anti-Flag M2 stained membranes with constructs used in this thesis, expressed in HEK293T cells. The membrane in Figure 6.A was subjected to immunostaining using an anti-GFP primary antibody, while the membrane in Figure 6.B was stained with an anti-Flag M2 primary antibody. Both membranes were treated with GAM secondary antibody. The membranes were visualised using the ECL Prime kit on ChemiDoc software. The sizes of the expressed proteins were compared to a Prestained Protein Ladder 10-180 kDa. Mock transfections included lysates obtained from cells not transfected with plasmid DNA. All cells used in the experiment were transfected with a 0.5 µg/mL concentration of plasmid DNA. The validity of the constructs was confirmed by conducting Western blot analysis in three independent repetitions.

4.2. Confirming previous results that TRIOBP-1 can co-aggregate with NDE1

After confirming the expression of constructs in mammalian cells, we aimed to replicate prior research outcomes. To achieve this, we used the SH-SY5Y human neuroblastoma cell line. Proteins of interest in this thesis have been cloned into either pDEST-CMV-N-EGFP or pdcDNA-Flag vectors which add an N-terminal EGFP fusion protein or a Flag tag, respectively. Proteins used in this part of the research were EGFP-TRIOBP-1 wild type, Flag-tagged NDE1, and EGFP control. EGFP control is an empty vector for control transfections that encodes EGFP (enhanced green fluorescent protein).

The constructs were transfected into SH-SY5Y cells and analysed by immunofluorescence microscopy. The primary purpose of performing single transfections of these proteins was to assess whether any of these proteins of interest aggregate independently, enabling comparison with their distribution when co-expressed with each other. In Figure 7.A we can see that EGFP control spreads out evenly across the cell. Figure 7.B shows a significant number of aggregates throughout the cell for EGFP-fused TRIOBP-1 wild type. Figure 7.C shows filamentous-like expression restricted to the body of the neuroblastoma cell (excluding the nucleus) for NDE1.

When testing the co-expression of Flag-tagged NDE1 with the EGFP control, NDE1 showed both co-aggregation and the normal expression pattern which was unexpected and not previously seen (Figures 8.A.1 and 8.A.2). In Figure 8.A.1., both signals are uniformly distributed throughout the cell, while in Figure 8.A.2., a clear co-aggregation is observed. Additionally, NDE1 demonstrated the formation of distinct co-aggregates when co-expressed alongside EGFP-TRIOBP-1. These aggregates were found to co-localize in the same positions, implying that TRIOBP-1 can potentially bind to NDE1, triggering its aggregation as well (Figure 8.B).

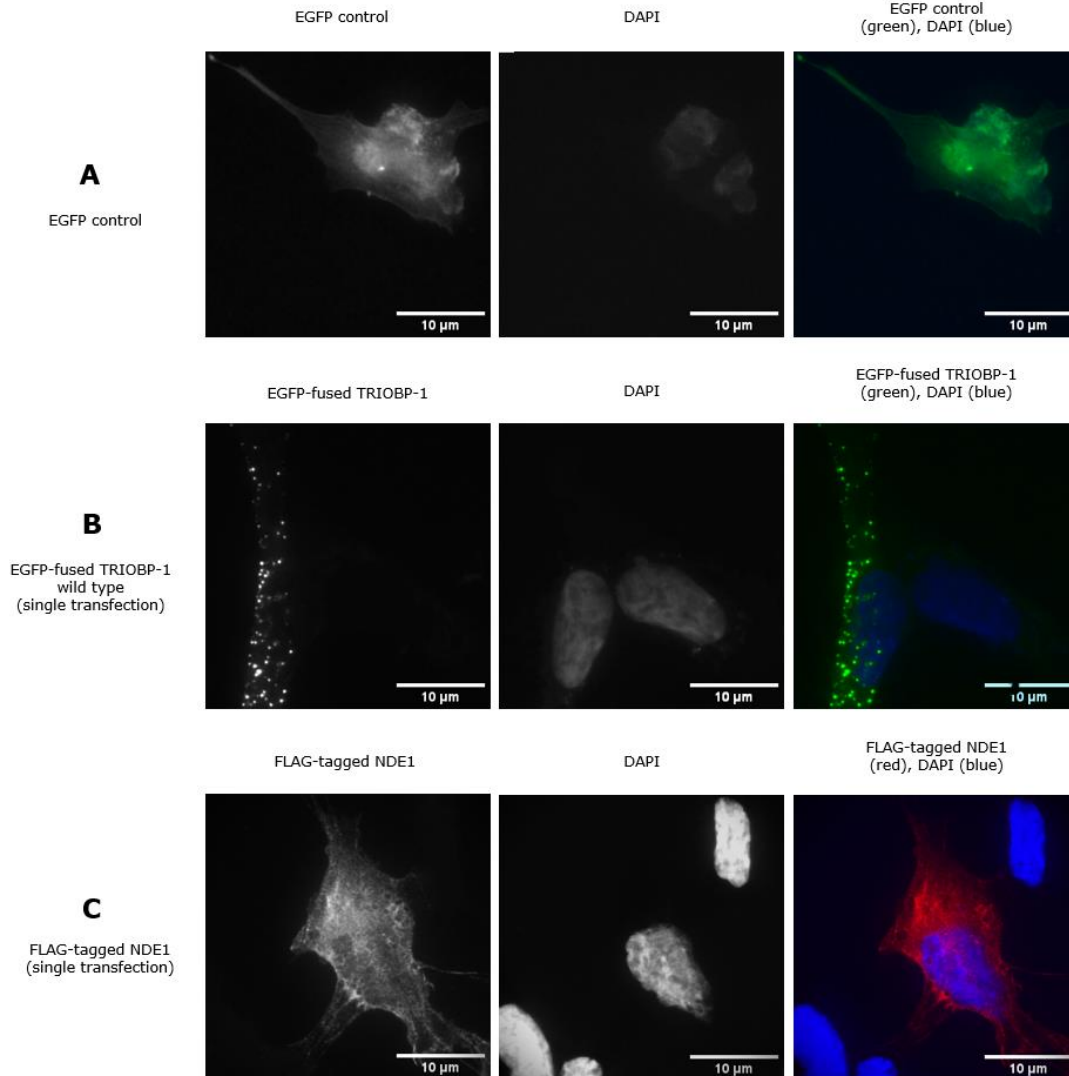


Figure 7: Single transfection controls. FLAG-tagged NDE1 in Figure 7.C was labelled with anti-Flag M2 primary antibody and GAM 555 nm secondary antibody, shown as a red signal. EGFP control in Figure 7.A and EGFP-TRIOBP-1 wild type in Figure 7.B were also stained with anti-Flag M2 primary antibody and GAM 555 nm secondary antibody as the control since the EGFP fluoresces on its own. DAPI was used to stain the nucleus blue. The images were captured under a fluorescent microscope at 60x magnification using the CellSens software. The scale bars in the images represent a length of 10 µm. EGFP control spreads out evenly across the cell. Flag-tagged NDE1 is evenly distributed in the cytoplasm of the cell. Wild type EGFP-TRIOBP-1 shows a significant number of aggregates throughout the cell. The constructs were analysed using fluorescent microscopy in three separate experiments.

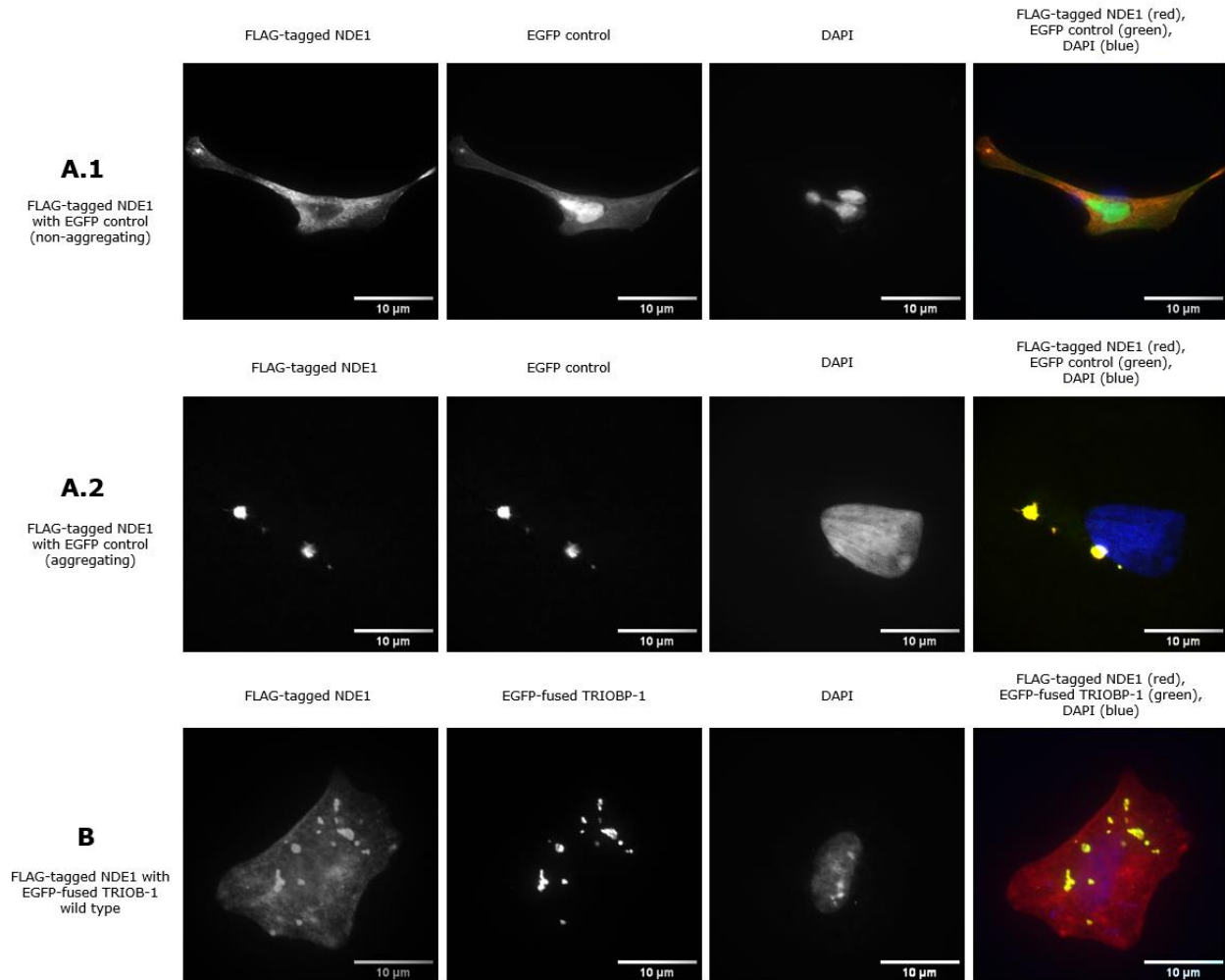


Figure 8: Replicating previous research results in SH-SY5Y cells with fluorescent microscopy. Flag-tagged NDE1 was labelled with anti-Flag M2 primary antibody and GAM 555 nm secondary antibody, while EGFP emits its own fluorescence. DAPI was used to stain the nucleus blue. The images were captured under a fluorescent microscope at 60x magnification using the CellSens software. The scale bars in the images represent a length of 10 μm. Figures **8.A.1** and **8.A.2** show the co-expression of Flag-tagged NDE1 and EGFP control. In Figure **8.A.1**, both signals are uniformly distributed throughout the cell, while in Figure **8.A.2**, a clear co-aggregation is observed. Co-expression of Flag-tagged NDE1 with wild type EGFP-TRIOBP-1 in Figure **8.B** also results in co-aggregation. The constructs were analysed using fluorescent microscopy in three separate experiments.

4.3. Co-aggregation of TRIOBP-1 and NDE1 is not dependent on the plasmid vectors used

Previous research results have been acquired by using a Flag-tagged NDE1 and EGFP-TRIOBP-1. Here in this step, we wanted to replicate the results but with switching vectors of the proteins and introducing the non-aggregating form of TRIOBP-1. This modified TRIOBP-1 version has had specific amino acids (1-59 and 333-340) deleted, effectively mitigating its propensity to aggregate³⁶.

In this part of the research, we used Flag-tagged TRIOBP-1 wild type and TRIOBP-1 (60-652, Δ 333-340) mutant, and NDE1 which has been cloned into a pDEST-CMV-N-EGFP vector. An EGFP control was used for comparative purposes, assessing its impact on protein aggregation due to its size.

Single transfections seen in Figure 9, have been done for the same reason as before – to discern whether any of the target proteins exhibit independent aggregation, preceding the investigation of their distribution when co-expressed.

In Figures 9.A and 9.B, shown in red, are Flag-tagged TRIOBP-1 wild type and TRIOBP-1 (60-652, Δ 333-340) mutant, respectively. As expected, the TRIOBP-1 wild type demonstrates abundant aggregates throughout the cell, whereas the mutant TRIOBP-1 (60-652, Δ 333-340) does not show signs of aggregation and exhibits uniform distribution. The EGFP control, seen in Figure 9.C, displays a natural even distribution. On the other hand, the EGFP-NDE1 surprisingly exhibits numerous structures resembling aggregates throughout the cell (Figure 9.D).

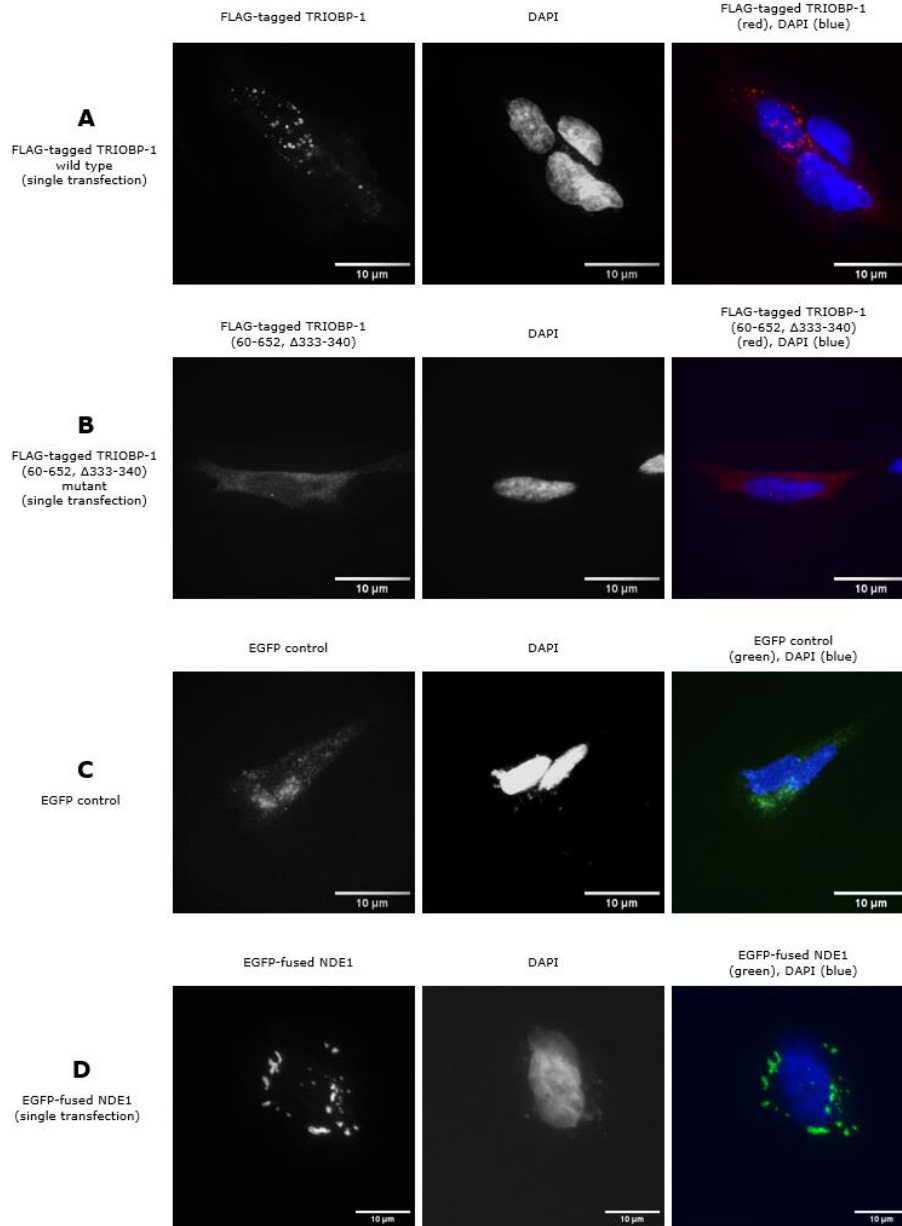


Figure 9: Single transfection controls for the experiment of switching vectors in NDE1 and TRIOBP-1 observed in SH-SY5Y cells with fluorescent microscopy. Flag-tagged wild type TRIOBP-1 and mutant TRIOBP-1 (60-652, Δ333-340) in **9.A** and **9.B** were labelled with anti-Flag M2 primary antibody and GAM 555 nm secondary antibody, appearing as a red signal. Similarly, the EGFP control and EGFP-NDE1 in **9.C** and **9.D** were stained with anti-Flag M2 primary antibody and GAM 555 nm secondary antibody as a control since EGFP emits fluorescence on its own. DAPI was used to stain the nucleus blue. The images were captured under a fluorescent microscope at 60x magnification using the CellSens software. The scale bars in the images represent a length of 10 μm. Wild type Flag-tagged TRIOBP-1 and EGFP-NDE1 displayed numerous aggregates throughout the cell, while mutant TRIOBP-1 (60-652, Δ333-340) and EGFP control were evenly distributed. The constructs were analysed using fluorescent microscopy in three separate experiments.

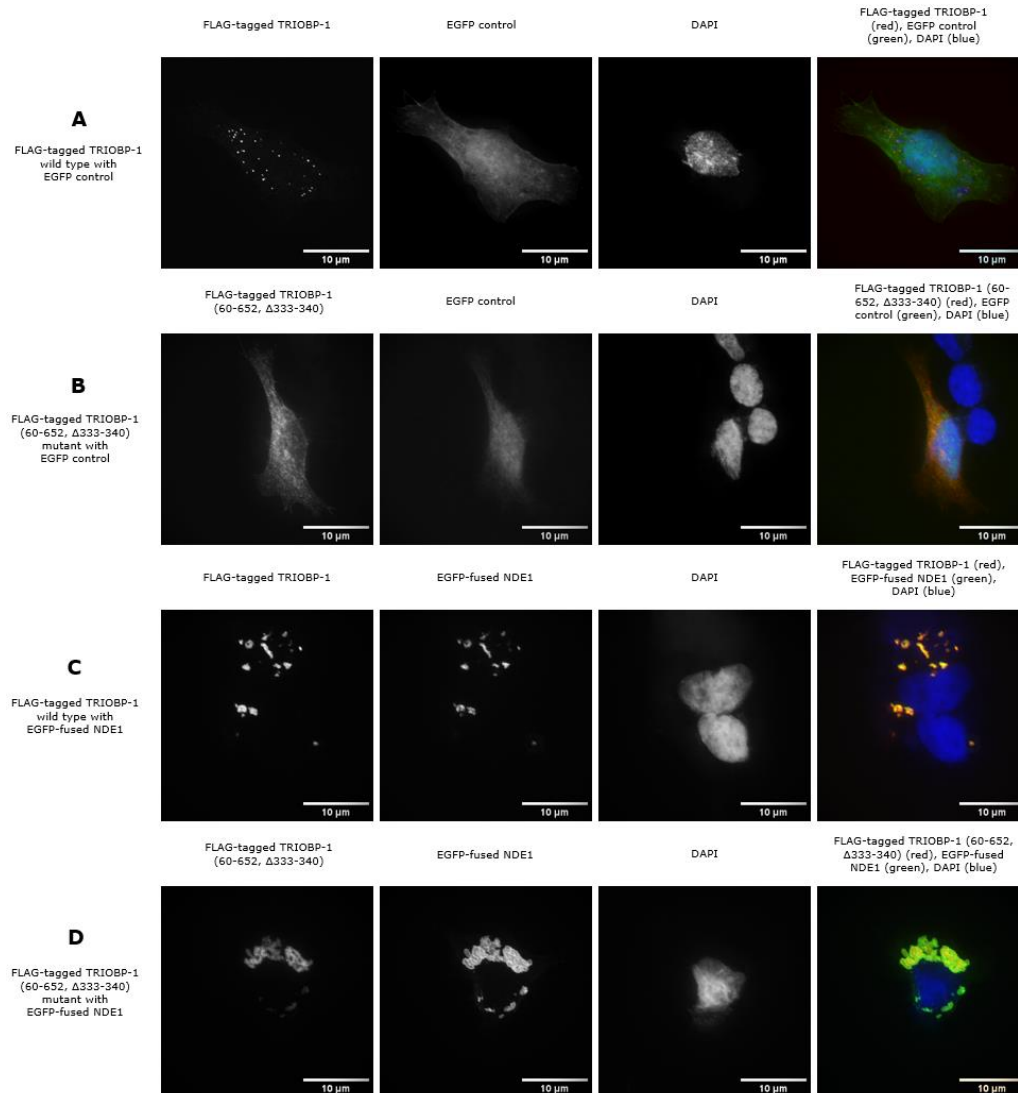


Figure 10: Switching vectors in NDE1 and TRIOBP-1 to observe the effect it has on the aggregation of those proteins in SH-SY5Y cells with fluorescent microscopy. Flag-tagged wild type TRIOBP-1 and mutant TRIOBP-1 (60-652, Δ333-340) were labelled with anti-Flag M2 primary antibody and GAM 555 nm secondary antibody, appearing as a red signal. The EGFP control and EGFP-NDE1 were also stained with anti-Flag M2 primary antibody and GAM 555 nm secondary antibody as the control, as EGFP emits fluorescence on its own. DAPI was used to stain the nucleus blue. The images were captured under a fluorescent microscope at 60x magnification using the CellSens software. The scale bars in the images represent a length of 10 μm. Co-expression of Flag-tagged wild type TRIOBP-1 and mutant TRIOBP-1 (60-652, Δ333-340) with EGFP control in figures **10.A** and **10.B** showed similar expression patterns as when they were individually transfected (Figure 9), suggesting that the presence of GFP does not affect their expression. Co-expression of EGFP-NDE1 with Flag-tagged wild type TRIOBP-1 and Flag-tagged mutant TRIOBP-1 (60-652, Δ333-340), shown in figure **10.C** and **10.D**, resulted in co-aggregation in both cases. The constructs were analysed using fluorescent microscopy in three separate experiments.

In this step of switching vectors in NDE1 and TRIOBP-1 to observe the effect it has on the aggregation of those proteins, SH-SY5Y cells were co-transfected with either an EGFP or Flag-tagged protein of interest together with another protein with the opposite tag. As previously mentioned, the proteins we used here were Flag-tagged TRIOBP-1 wild type and TRIOBP-1 (60-652, Δ 333-340) mutant, and an EGFP-NDE1 as well as an EGFP control. The EGFP control was used to eliminate the potential influence of GFP itself on the expression of the protein of interest.

Co-expression of Flag-tagged wild type TRIOBP-1 and mutant TRIOBP-1 (60-652, Δ 333-340) with EGFP control in Figures 10.A and 10.B showed similar expression patterns as when they were individually transfected (Figure 9). This observation suggests that the presence of GFP does not affect their expression. In Figure 10.C, as expected, a clear co-aggregation is observed between EGFP-NDE1 and Flag-tagged wild type TRIOBP-1. On the other hand, co-expression of EGFP-NDE1 with a non-aggregating Flag-tagged mutant TRIOBP-1 (60-652, Δ 333-340), shown in Figure 10.D, unexpectedly, also resulted in co-aggregation.

4.4. NDE1 is insoluble in the cell, suggesting it may aggregate

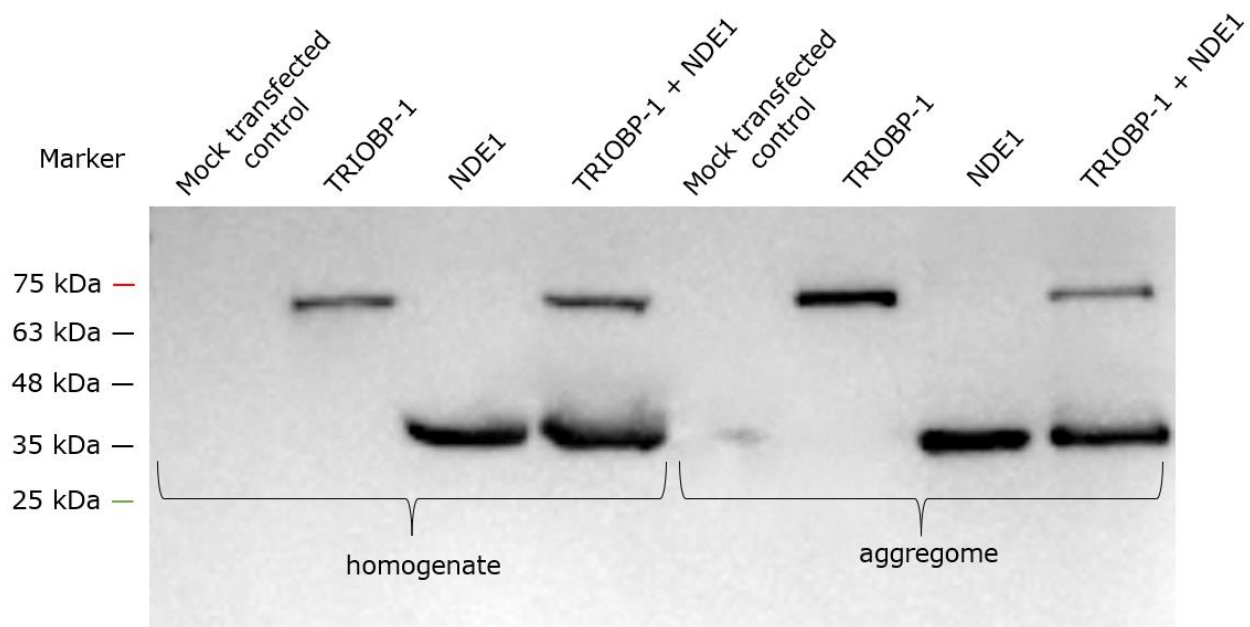
Up until this point, our primary focus involved introducing plasmid constructs into SH-SY5Y cells and assessing outcomes through visual analysis. Guided by visual observations, these plasmid constructs were categorized based on their aggregation behaviour—classified as aggregating or non-aggregating. In order to ascertain the true nature of the spotted formations, described as aggregates, and to confirm whether they genuinely constitute insoluble proteins, we conducted an aggregome purification assay.

After the surprising finding of NDE1 aggregation, we have decided to do the insoluble fraction purification assay to check whether its aggregation and co-aggregation with TRIOBP-1 is related to the role of NDE1 as a tubulin-binding protein. We hypothesised that the aggregates we see are not aggregates as such but are clumps of NDE1 bound to tubulin, or a combination of both. If the latter is the case, there should be a NDE1 band in the aggregome part of the Western blot.

The insoluble fraction purification assay was done as previously described in section 3.2.11. Here, we used Flag-tagged TRIOBP-1 wild type and Flag-tagged NDE1. HEK293T cells were either single-transfected with Flag-tagged TRIOBP-1 wild type or Flag-tagged NDE1, or co-transfected with aforementioned protein plasmids. As a control, mock-transfected HEK293T cells were included. Following the overnight incubation, the cells were lysed, homogenate samples were taken, and the rest of the lysate was used in the assay. Cell lysates' insoluble portions were isolated using a modified protocol involving multiple steps of centrifugation and resuspension in different buffers. The most insoluble proteins were contained in the final pellet at the bottom of the UC tube. The obtained insoluble pellets were subsequently dissolved, processed, and stored for later Western blot analysis. Samples of original lysates (homogenate) and their purified insoluble fractions (aggregome) were examined by Western blot (Figure 11). The proteins were detected using an anti-FLAG M2 primary antibody and GAM secondary antibody.

The following blot, seen in Figure 11, shows the results of the protein purification assay. On the left side of the blot are the samples from the homogenate fraction and their levels of expression in the lysate, whereas on the right are the purified samples from the aggregome fraction containing the insoluble protein. Notable differences in expression levels across proteins under these two conditions are not evident. TRIOBP-1, previously identified as aggregating³⁰, exhibits a visibly higher expression within its insoluble

fraction, signifying the persistence of the insoluble fraction from the original sample during the procedure. On the other hand, NDE1, categorized as non-aggregating, reveals no significant expression variations between the homogenate and aggregome fractions. This suggests that some protein did not completely dissolve. This could be due to the solubilization buffers not working optimally or because a portion of NDE1 existed as aggregates, aligning with our prior findings in Figures 8.A.2, 9.D, and 10.C and D. It's worth noting that a negative control could provide further clarity in confirming these observations.



Primary antibody: anti-FLAG M2

Figure 11: Ultracentrifugation assay revealed the insolubility of both single transfected TRIOBP-1 and NDE1, and their co-aggregates. Constructs used in this assay were Flag-tagged TRIOBP-1 wild type and Flag-tagged NDE1. The proteins were detected using an anti-FLAG M2 primary antibody and GAM secondary antibody. As a control, mock-transfected HEK293T cells were included. The sizes of the proteins were compared to a Prestained Protein Ladder 10-180 kDa. The proteins present in the aggregome fraction underwent ultracentrifugation, while those in the homogenate fraction did not. The obtained results were confirmed in three independent repetitions.

4.6. Testing protein insolubility after nocodazole treatment

To delve deeper into our hypothesis that the aggregates of NDE1 are not aggregates as such, but are clumps of NDE1 bound to tubulin, or a combination of both, we have treated cells with nocodazole. Nocodazole, an anti-mitotic agent, interacts with beta-tubulin and disrupts microtubule assembly/disassembly dynamics by hindering microtubule polymerization.

Plasmid constructs used here are the same as the ones used in the previous experiment - Flag-tagged TRIOBP-1 wild type and Flag-tagged NDE1. Mock-transfected HEK293T cells were included as a control. Preceding to insoluble protein purification assay, transfected or mock transfected HEK293T cells were treated with nocodazole diluted in DMSO and incubated at 4°C (Figure 12.C). Two control plates were set up: Figure 12.A depicts protein expression levels of homogenate and aggregate fractions from control cells treated with DMSO, followed by incubation at 37°C, while Figure 12.B shows the same for cells incubated at 4°C. Following the incubations, the assay was performed in the same manner as previously described (section 3.2.11.) The proteins were detected using an anti-Flag M2 primary antibody and GAM secondary antibody.

It's important to note that the observed subtle variations in expression levels between the two control conditions and the nocodazole-treated cells, as well as the minor expression differences between their homogenate and aggregate fractions, require further quantification. This outcome provides initial support for the presence of NDE1 in aggregate-like formations. However, it's crucial to recognize that this conclusion is preliminary, as we did not include a positive control for the nocodazole treatment to confirm whether tubulin was indeed breaking down. Moreover, the observed reduction in insoluble NDE1 after nocodazole treatment suggests that the insoluble NDE1

likely comprises both NDE1 bound to tubulin and aggregating NDE1, but further experiments are needed for confirmation.

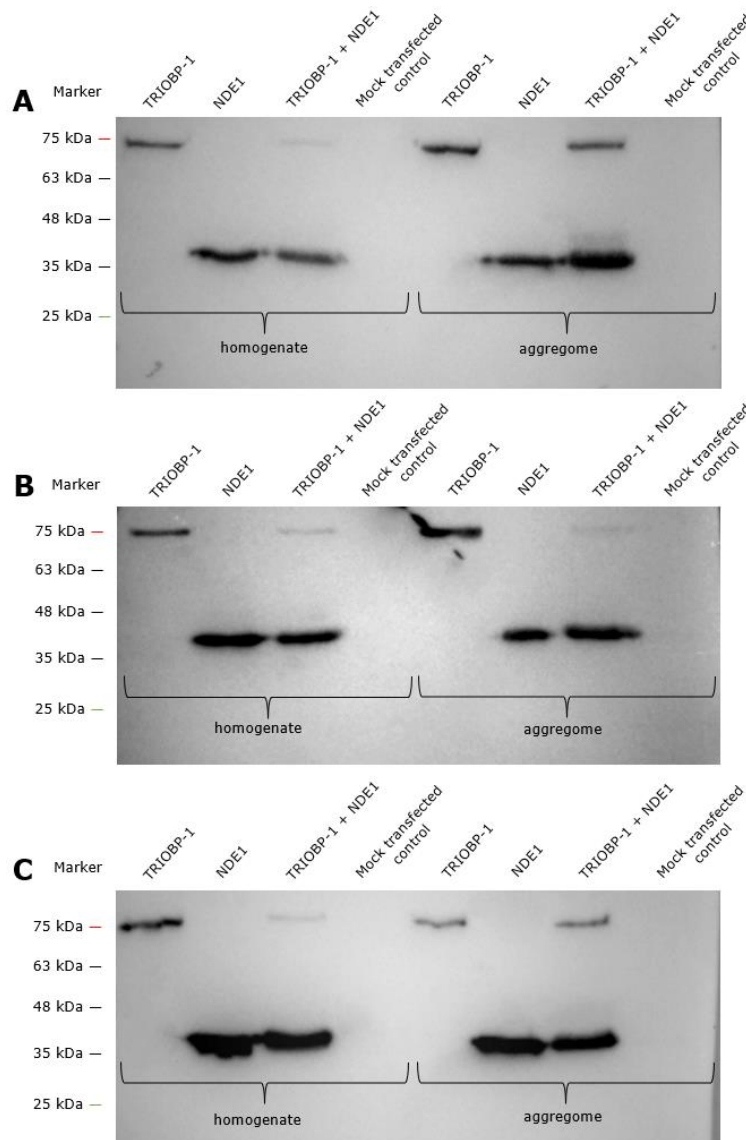


Figure 12: The ultracentrifugation assay was performed after treating cells with nocodazole to assess its effect on the aggregome of NDE1 specifically. Constructs used in this assay were Flag-tagged TRIOBP-1 wild type and Flag-tagged NDE1. Figures **12.A** and **12.B** represent the protein expression levels in control cells treated with DMSO, which were then incubated at 37°C or at 4°C, respectively. Figure **12.C** shows proteins after the ultracentrifugation assay from cells treated with nocodazole diluted in DMSO and incubated at 4°C. The proteins were detected using an anti-Flag M2 primary antibody and GAM secondary antibody. Mock transfected HEK293T cells were included as a control. The sizes of the proteins were compared to a Prestained Protein Ladder 10-180 kDa. The proteins present in the aggregome fraction underwent ultracentrifugation, while those in the homogenate fraction did not.

4.5. NDE1 and NDEL1 behave similarly in HEK293T cells to SH-SY5Y cells

Given that our immunofluorescence assays were performed in SH-SY5Y cells, but our insolubility assays were performed in HEK293, it is possible that the results cannot be directly compared. We therefore repeated our immunofluorescence assays in HEK293 cells, to check that our proteins behaved similarly to in SH-SY5Y cells.

Figure 13 displays the results of single transfections of EGFP control, EGFP-TRIOBP-1, and Flag-tagged NDE1. The distribution patterns of these proteins match their original descriptions: EGFP control and Flag-tagged NDE1, shown in Figures 13.A and 13.C, respectively, are evenly spread across the cell, while EGFP-TRIOBP-1 in Figure 13.B naturally forms visible aggregates.

In Figure 14, we confirm the observations made in the SH-SY5Y cell line. Figures 14.A and 14.B depict two scenarios involving co-transfection of Flag-tagged NDE1 and EGFP control. In the first scenario, both plasmids show an even distribution, with EGFP control having a slightly greater presence in the nucleus, and Flag-tagged NDE1 being evenly distributed in the cell's cytoplasm. In the second scenario, co-aggregation of the two proteins is evident, with both being localized around the nucleus. Additionally, Figure 14.B confirms the co-aggregation of EGFP-TRIOBP-1 and Flag-tagged NDE1 once again.

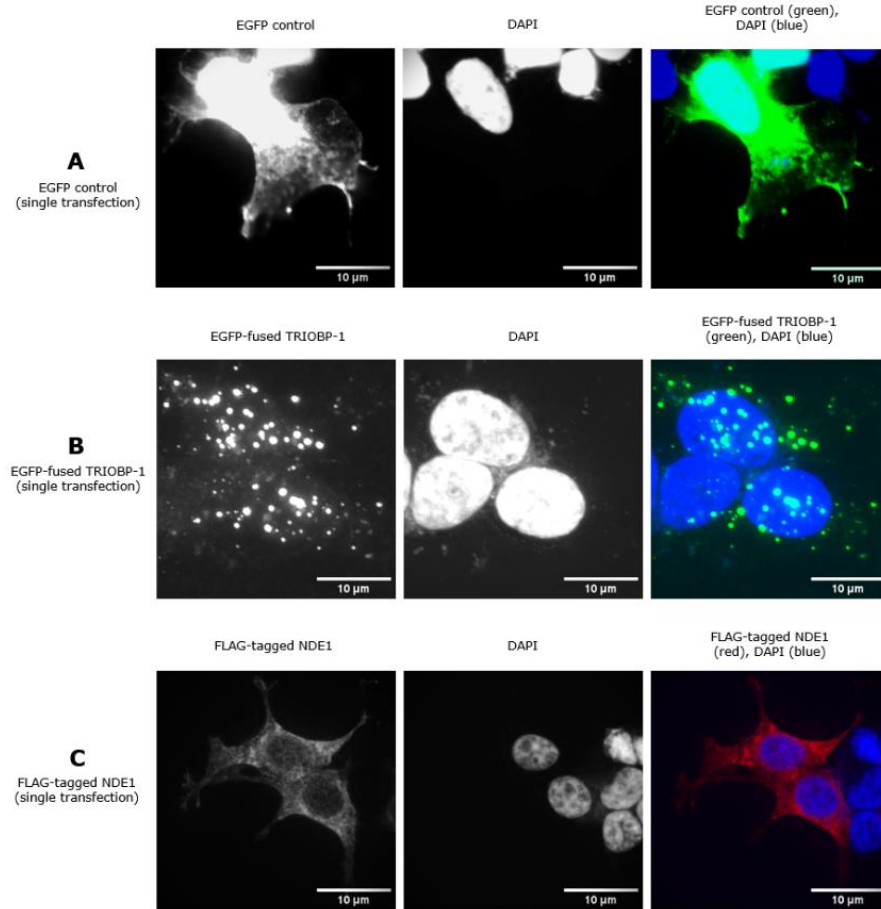


Figure 13: Controls for expressing NDE1 and TRIOBP-1 plasmids in HEK293T. Flag-tagged NDE1 was labelled with anti-Flag M2 primary antibody and GAM 555 nm secondary antibody, appearing as a red signal. EGFP control and EGFP-TRIOBP-1 were also stained with anti-Flag M2 primary antibody and GAM 555 nm secondary antibody as the control, as EGFP emits fluorescence on its own. DAPI was used to stain the nucleus blue. The images were captured under a fluorescent microscope at 60x magnification using the CellSens software. The scale bars in the images represent a length of 10 µm. EGFP and Flag-tagged NDE1 show an even distribution throughout the cell and cytoplasm, respectively. EGFP-TRIOBP-1 displayed numerous aggregates throughout the cell. The constructs were analysed using fluorescent microscopy in three separate experiments.

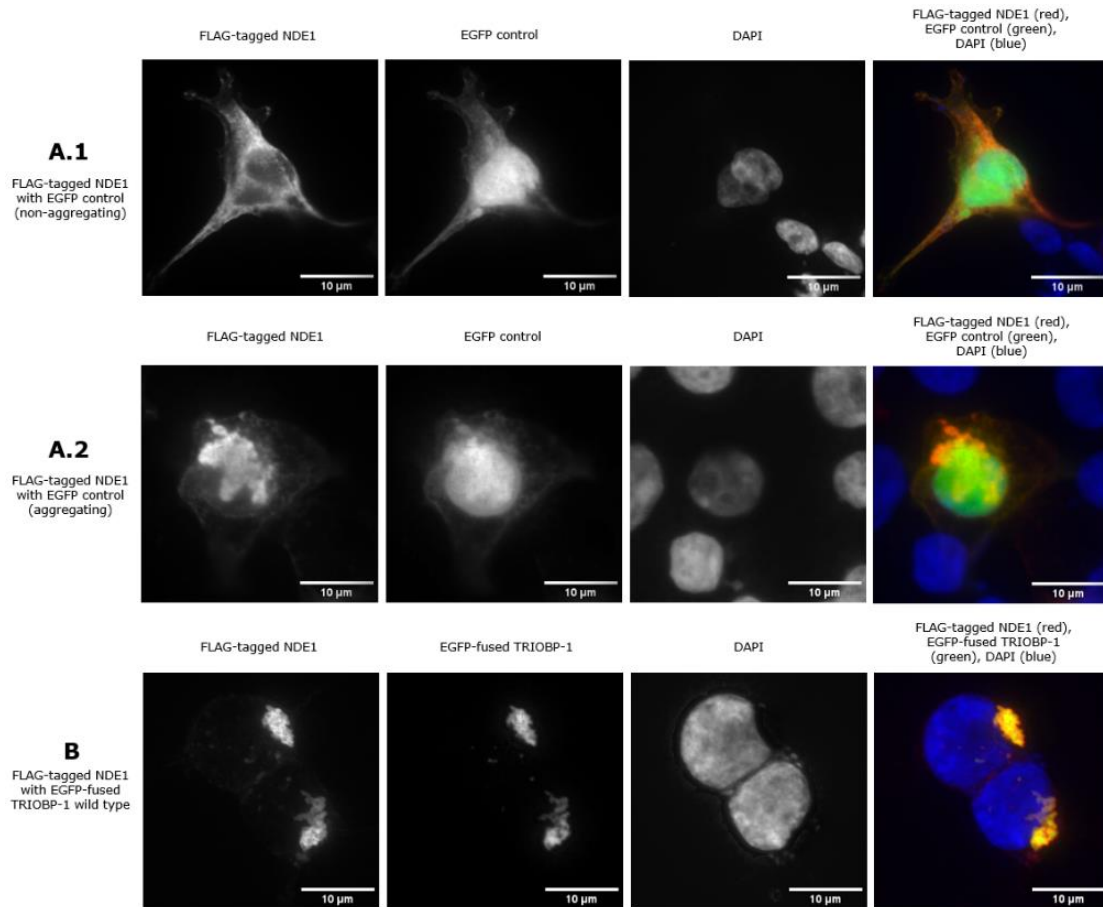


Figure 14: Expressing NDE1 and TRIOBP-1 plasmids in HEK293T to check if aggregation propensity changes by changing a cell line. Flag-tagged NDE1 was labelled with anti-Flag M2 primary antibody and GAM 555 nm secondary antibody, appearing as a red signal. EGFP control and EGFP-TRIOBP-1 were also stained with anti-Flag M2 primary antibody and GAM 555 nm secondary antibody as the control, as EGFP emits fluorescence on its own. DAPI was used to stain the nucleus blue. The images were captured under a fluorescent microscope at 60x magnification using the CellSens software. The scale bars in the images represent a length of 10 μm . In **14.A.1** and **14.A.2** co-transfection of Flag-tagged NDE1 and EGFP control is shown. In **14.A.1** both NDE1 and EGFP are showing an even distribution throughout the cell. In **14.A.2** co-aggregation of the aforementioned proteins can be seen. Figure **14.B** shows clear co-aggregation of Flag-tagged NDE1 and EGFP-TRIOBP-1 wild type. The constructs were analysed using fluorescent microscopy in three separate experiments.

5. Discussion

Certain conditions like major depressive disorder, bipolar affective disorder, and schizophrenia fall under the category of chronic mental illnesses (CMIs) due to their persistent or recurring nature throughout a person's life. CMIs profoundly affect individuals by directly influencing their emotions, thoughts, and behaviours. The complexity of their origins and mechanisms has led to a limited understanding of their nature. Given that CMIs are among the leading global causes of disability, increased awareness has prompted researchers to focus on uncovering the underlying biological factors contributing to these disorders' development. CMIs are a complex challenge in the field of mental health, with conditions like schizophrenia highlighting the struggle. Schizophrenia is a globally spread disorder that lacks proper diagnosis and effective treatment options. This gap in our understanding demands fresh approaches. While progress has been made, we're still in the dark about what exactly causes schizophrenia, and standard ways of diagnosing and treating it aren't enough. In the midst of this complexity, there's a new aspect of research that holds promise for understanding the disorder on a deeper level, and that is protein aggregation.

This research focuses on protein aggregation, a process where misfolded proteins accumulate to form insoluble complexes or aggregates and disrupt normal cellular processes. These aggregates are linked to various diseases, from neurodegenerative disorders to metabolic issues. Connecting protein aggregation to schizophrenia offers a different angle beyond the usual genetic explanations. Investigating how protein aggregation contributes to schizophrenia could discover potential non-genetic factors at play in the disorder's development. This fresh perspective holds the promise of transforming our comprehension of schizophrenia, potentially leading to more precise targets and new treatments that address its molecular aspects.

5.1 Co-aggregation of TRIOBP-1 and NDE1

This research project focused on delving into the interaction dynamics of TRIOBP-1 and NDE1. Notably, NDE1, a protein associated with (CMIs), exhibited consistent expression in SH-SY5Y cells. Intriguingly, when co-expressed with TRIOBP-1, it sparked the formation of aggregates, implying its potential role as a co-aggregation partner in CMIs, particularly in the context of schizophrenia. This alignment of NDE1 and TRIOBP-1 in their functional roles is in sync with their established functions in neurodevelopment and oligodendrocyte differentiation. Building upon earlier investigations involving TRIOBP-1 and NDE1, this thesis pursued several main objectives to validate the co-aggregation phenomenon between wild-type TRIOBP-1 and NDE1, using alternative vectors for a comprehensive exploration. The research also aimed to investigate the potential aggregation instigation resulting from the co-expression of NDE1 with mutated non-aggregating TRIOBP-1. Additionally, the study sought to explore the possible connection between the co-aggregation of NDE1 and TRIOBP-1 and the role of NDE1 as a tubulin-binding protein.

Based on previous research which proposed that the aggregation mechanism implicating TRIOBP-1 misassembly is responsible for recruiting NDE1 to co-aggregate and confirmed the co-aggregation of TRIOBP-1 and NDE1³⁷, we have decided to replicate these results and deepen the research a bit more.

After verifying all our plasmids and their expression levels by Western blot (Figure 6), we wanted to investigate whether these expressed proteins formed visible aggregates in cell culture by themselves or are they able to recruit each other to aggregate, and to do so, we overexpressed them in the SH-SY5Y human neuroblastoma cell line. Single transfections of the aforementioned plasmids were in line with previous results and descriptions – the EGFP control was evenly distributed throughout the whole cell, EGFP-TRIOBP-1 has shown

numerous aggregates, and lastly, NDE1 exhibited a filamentous-like expression restricted to the body of the neuroblastoma cell (Figure 7). Next, we have co-expressed the EGFP control with Flag-tagged NDE1, to exclude any effect it may have on NDE1's aggregation propensity because of its size, and EGFP-TRIOBP-1 with Flag-tagged NDE1 as was done in previous research. When co-expressed with EGFP-TRIOBP-1, Flag-tagged NDE1 had demonstrated the formation of distinct co-aggregates, as seen in Figure 8.B, although NDE1 has kept some of its normal distribution. These aggregates were found to co-localize, confirming the hypothesis of the potential TRIOBP-1 has on triggering NDE1's aggregation. Additionally, an unexpected result was seen in Figures 8.A.1 and 8.A.2. when testing the co-expression of Flag-tagged NDE1 with the EGFP control, NDE1 showed both co-aggregation and a normal expression pattern which was surprising and not previously seen. In the first situation of no aggregation as seen in Figure 8.A.1, both signals are uniformly distributed throughout the cell, while in Figure 8.A.2, a clear co-aggregation and co-localization is observed. The same trend of partial co-aggregation was again seen later on in the HEK293T cell line, as shown in Figures 14.A.1 and 14.A.2 confirming that the tendency of the EGFP control and Flag-tagged NDE1 does not change by changing the cell line.

As the next step, we wanted to replicate the results but with switching vectors of the proteins to investigate the behaviour of NDE1 fused with EGFP and to introduce the non-aggregating form of TRIOBP-1. This mutant of TRIOBP-1 has had specific amino acids (1-59 and 333-340) deleted, effectively diminishing its propensity to aggregate³⁶. To do this we first needed to generate the EGFP-NDE1, which was accomplished using the LR clonase recombination reaction. The full-length human NDE1 was transferred into the destination vector pDEST-CMV-N-EGFP using the Gateway cloning system. The recombination process resulted in the formation of a final construct in the destination vector - NDE1 with an EGFP fusion protein at its N-terminus which

was confirmed by sequencing. In this part of the research, we used Flag-tagged TRIOBP-1 wild type and TRIOBP-1 (60-652, Δ 333-340) mutant, newly generated EGFP-NDE1 and EGFP control again for comparative purposes. Single transfections of plasmids in switched vectors we did to discern whether any of the target proteins exhibit independent aggregation, preceding the investigation of their distribution when co-expressed. Flag-tagged TRIOBP-1 wild type and TRIOBP-1 (60-652, Δ 333-340) mutant followed the trend of their previous research, that is, the wild type has demonstrated abundant aggregates throughout the cell, whereas the mutant did not show signs of aggregation and has exhibited a uniform distribution (Figures 9.A and 9.B, respectively). The EGFP control by itself naturally shows an even distribution as seen in Figure 9.C. Moreover, to our surprise, EGFP-NDE1, in Figure 9.D, has exhibited numerous aggregates throughout the cell. Subsequently, after conducting single transfections, the study progressed to perform co-transfections of the specified plasmids. In this phase, co-expression of Flag-tagged wild type TRIOBP-1 and mutant TRIOBP-1 (60-652, Δ 333-340) with the EGFP control in Figures 10.A and 10.B displayed similar expression patterns to their individual transfections (Figure 9). This finding suggests that the presence of GFP does not impact their expression. In Figure 10.C, the anticipated outcome emerged with clear co-aggregation observed between EGFP-NDE1 and Flag-tagged wild type TRIOBP-1. Conversely, Figure 10.D unveiled an unexpected result—co-expression of EGFP-NDE1 with a non-aggregating Flag-tagged mutant TRIOBP-1 (60-652, Δ 333-340) also led to co-aggregation.

Table 5: List of used and related plasmids and their tendency to aggregate when over-expressed

Plasmid	Tendency to aggregate when over-expressed
FLAG-tagged TRIOBP-1 wt* (652 aa)	Yes
EGFP-fused TRIOBP-1 wt (652 aa)	Yes
FLAG-tagged TRIOBP-1 mt* (60-652, Δ 333-340)	No
EGFP-fused TRIOBP-1 mt (60-652, Δ 333-340)	Unknown (the protein is unstable)
FLAG-tagged NDE1	No
EGFP-fused NDE1	Yes
EGFP control	No
EGFP control w/ FLAG-tagged NDE1	Co-aggregation
FLAG-tagged TRIOBP-1 wt w/ EGFP-fused NDE1	Co-aggregation
EGFP-fused TRIOBP-1 wt w/ FLAG-tagged NDE1	Co-aggregation
FLAG-fused TRIOBP-1 mt w/ EGFP-tagged NDE1	Co-aggregation
EGFP-fused TRIOBP-1 mt w/ Flag-tagged NDE1	Unknown

* wt = wild type, mt = mutant

5.2 NDE1 as a potential aggregating protein

After several surprising results so far, it is needed to delve into the discussion of the EGFP-NDE1 aggregation. From a single transfection of EGFP-NDE1 in Figure 9.D it appears that NDE1 can aggregate, at least under some circumstances, which was previously thought otherwise. While there are no published results about NDE1 aggregating by itself, our findings here seem to be consistent with the unpublished results from Bradshaw *et al.* who have captured needle-like NDE1 aggregates which were negatively stained and visualized by electron micrograph (Figure 15). It is currently unknown if this aggregation is relevant to disease or not. Figure 16 represents what the normal molecules of NDE1 look like.

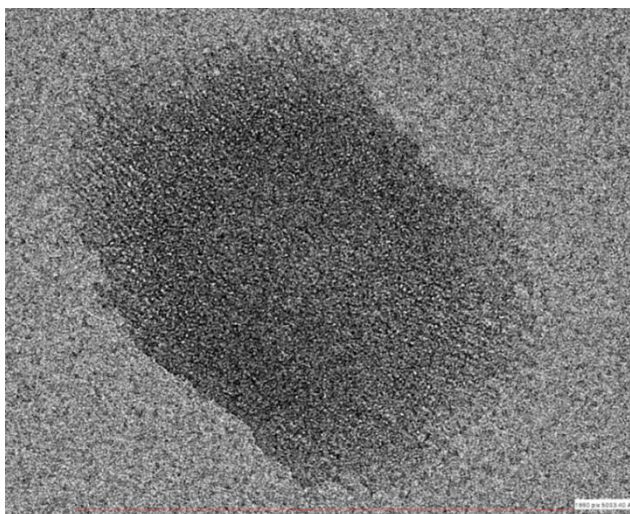


Figure 15: NDE1 aggregates. The image represents filamentous-like NDE1 aggregates negatively stained and visualized by electron microscopy. Unpublished, taken from Bradshaw *et al.*

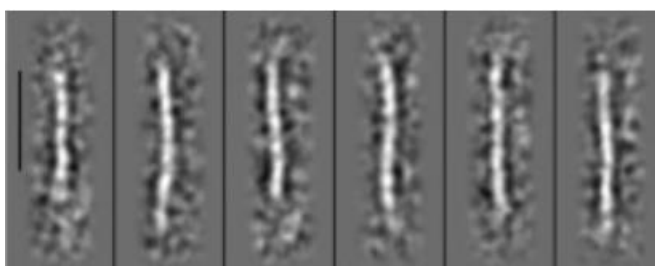


Figure 16: NDE1 molecules. This image shows what the normal molecules of NDE1 look like visualised by electron microscopy. Scale bar, 20 nm. Taken from Soares *et al.*⁴⁷.

The fact that EGFP-NDE1 aggregates and Flag-tagged NDE1 does not, brings us to our next problem. Our current hypothesis is that NDE1 is naturally somewhat inclined to aggregation, but the cell is normally able to handle it and degrade the protein that begins to aggregate before it becomes a major issue. By adding EGFP, which is known to stabilise proteins in the sense that it prevents proteins from being degraded as quickly, we stabilise the expression of NDE1, meaning that the cell can no longer deal with it and degrade it by the proteasome. The EGFP control is an empty vector used for control transfections which encodes EGFP (enhanced green fluorescent protein) and is fairly big in size (~30 kDa). The results showing that EGFP-NDE1 is more aggregation prone than Flag-tagged NDE1 suggest that NDE1 is actively degraded if it starts to aggregate, but that the EGFP prevents this. A very similar effect was seen with another protein implicated in schizophrenia, CRMP1, where it was notable that CRMP1 had showed an increased tendency to aggregate when fused to EGFP⁴⁴. This would potentially explain the fact that Flag-tagged NDE1 was insoluble but did not form visible aggregates. The insolubility assay is sensitive to early-stage misfolded protein before the aggregates are visible.

Another thing important to address regarding NDE1 and EGFP is the co-aggregation of Flag-tagged NDE1 and the EGFP control which happens partially. Figure 17 encompasses both situations in one field of view, no co-aggregation, and visible co-aggregates, in two cells one next to the other. Flag-NDE1 and EGFP co-aggregation is unexpected, but in short, suggests that NDE1 can bind to EGFP. The fact that EGFP does not aggregate alone, while NDE1 does in some circumstances, suggests that NDE1 is potentially initiating the co-aggregation, although this is not yet confirmed. It is unclear why this is seen here but was not seen in previous experiments. The reason for this could be because of differences in temperature in the lab, which can be

causing additional stress on NDE1 in this experiment, further research into this is necessary.

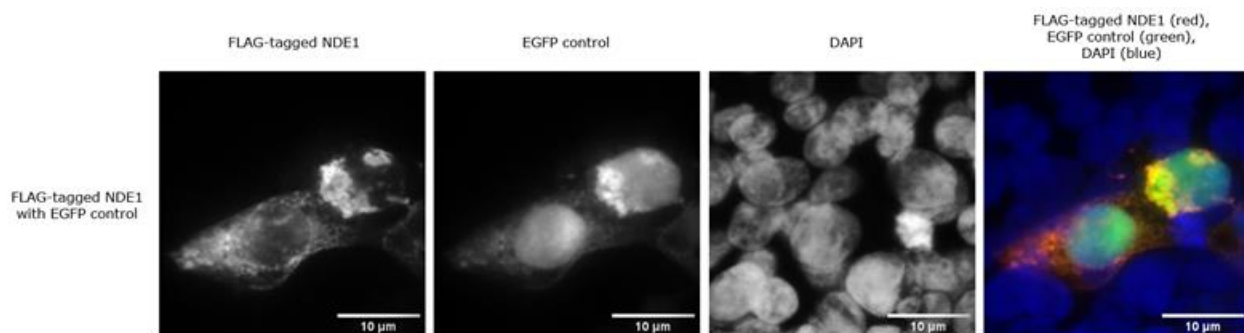


Figure 17: NDE1 co-expressed with EGFP control in HEK293T cell line. Constructs used in this assay were Flag-tagged NDE1 and EGFP control. Flag-tagged NDE1 was labelled with anti-Flag M2 primary antibody and GAM 555 nm secondary antibody, appearing as a red signal. EGFP emits fluorescence on its own. DAPI was used to stain the nucleus blue. The images were captured under a fluorescent microscope at 60x magnification using the CellSens software. The scale bars in the images represent a length of 10 µm. In these two cells, NDE1 is both co-aggregating and not with EGFP control. The constructs were analysed using fluorescent microscopy in three separate experiments.

The subsequent aspect to be addressed involves the co-aggregation of NDE1 and TRIOBP-1. Existing evidence demonstrates that NDE1 has the ability to co-aggregate with TRIOBP-1. This occurs regardless of the tags attached to each protein, strongly indicating a specific interaction between NDE1 and TRIOBP-1. This inference is further supported by the known interaction between NDEL1 and TRIOBP-1⁴⁶. Therefore, it would not be unexpected for NDE1 and TRIOBP-1 to interact in their functional forms as well. Nonetheless, the fact that NDE1 can also interact with EGFP introduces a degree of uncertainty. Moreover, the interaction of NDE1 with two proteins associated with schizophrenia-related aggregation (TRIOBP-1 and DISC1) underscores the need for a more comprehensive investigation. Notably, the findings that NDE1 aggregates selectively under certain conditions and with specific constructs suggest a delicate stability balance, allowing it to transition into aggregation with ease. Another unexpected finding is NDE1's co-aggregation with a non-aggregating mutant TRIOBP-1. This surprising observation implies that NDE1 can induce the aggregation of the TRIOBP-1 mutant. Interestingly,

a similar mechanism was recently discovered for DISC1 and mutant TRIOBP-1. Samardžija et al.'s study revealed that the TRIOBP-1 mutant, which didn't aggregate alone or with EGFP, did co-aggregate with full-length DISC1 in certain cells. This implies that the co-aggregation of these proteins could be driven primarily by DISC1's inherent aggregation propensity, suggesting a distinct mechanism from TRIOBP-1's individual aggregation process⁴⁴. Nevertheless, the results for this thesis of NDE1 and TRIOBP-1 mutant's co-aggregation still need to be confirmed by co-expressing the Flag-tagged NDE1 with a non-aggregating TRIOBP-1 mutant fused with EGFP. This was attempted before and although the mutant exhibited the anticipated size upon transfection into HEK293T cells and Western blot analysis, it also displayed aggregation tendencies. Again, this could potentially be attributed to the EGFP-fused protein itself as is the case with NDE1. Regrettably, the outcomes derived from the co-expression of this protein combination do not yield dependable results.

The last step of this research was conducting the insolubility assay. Herein we wanted to distinguish if the aggregates we see under the microscope are indeed insoluble aggregates or tubulin-bound NDE1, specifically. In this assay, we used Flag-tagged TRIOBP-1 wild type and NDE1, which were over-expressed in HEK293T cells independently and together. The cells were lysed and subjected to a sequence of solubilization buffers, followed by centrifugation. The result seen in Figure 11, supports our findings. This is particularly seen in the aggregome fraction on the blot, where there is a very high level of insoluble NDE1 when expressed alone. The insolubility assay was repeated but with the treatment of cells with nocodazole prior to the lysis step. In Figure 12.C it is visible that there is less insoluble NDE1 in the aggregome relative to the NDE1 in the homogenate fraction. It's worth mentioning that while it is certainly a possibility that the observed clumps are related to NDE1 aggregation, there is a higher probability that NDE1 was insoluble in the

insolubility assay because it was bound to actin. The insolubility assay primarily detects insoluble proteins, and protein aggregation is a major reason for a protein to be insoluble. However, it's essential to consider that binding to the cytoskeleton, particularly actin, could potentially contribute to this insolubility. Further experiments are needed to clarify the precise nature of these insoluble formations.

5.3. Future research directions

It is evident that the research of NDE1 and TRIOBP-1 co-aggregation needs to be continued. Firstly, to check if in the case of co-transfection of FLAG-tagged NDE1 and EGFP control co-aggregation really occurs or if those are exceptions, quantification should be done. Ideally, the next step would also be to co-transfect FLAG-tagged NDE1 and the EGFP-TRIOBP-1 mutant (60-652, Δ 333-340). As mentioned before, the experiment was already attempted, but although it was confirmed to be the right protein, the non-aggregating EGFP-TRIOBP-1 mutant (60-652, Δ 333-340) is aggregating.

Furthermore, to overcome the issue of proteins aggregating in the presence of EGFP, the idea would be to remove EGFP from this altogether. The solution for this would be to select another small tag like V5 or something like it and closer to Flag in size, put our proteins into this and then co-express them with Flag-tagged proteins.

After looking into NDE1 and TRIOBP-1 co-aggregation with different vectors, the next thing that can be investigated is which regions of TRIOBP-1 are involved in NDE1 interaction/co-aggregation. By employing the non-aggregating TRIOBP-1 mutant, we could confirm the significance of the TRIOBP-1 aggregation motif in NDE1 co-aggregation. Demonstrating that this region isn't responsible for NDE1 aggregation would prompt further investigations, including examining NDE1 expression when co-transfected with TRIOBP-1 variants featuring different deleted regions.

Identifying the specific TRIOBP-1 region responsible for NDE1 co-aggregation and whether it disrupts its protein folding and role in neurodevelopment, we would be able to design additional experiments, deepening our understanding of how protein co-aggregation contributes to the mechanism and non-genetic onset of schizophrenia.

When important parts of brain cells are disrupted—such as how they stabilize their structure or form connections—it can disrupt the balance of chemicals that transmit signals in the brain. This disruption is known in conditions like schizophrenia. So, TRIOBP-1 and NDE1 coming together might uncover a way that schizophrenia could start, showing a specific part of what's different in the brains of people with this disorder.

6. Conclusion

As our understanding of chronic mental illnesses (CMIs) improves and diagnostic methods become more refined, research into their complex molecular dynamics has gained increasing importance. CMIs pose diagnostic and treatment challenges due to their complexity. Recent insights have linked protein aggregation, including proteins like TRIOBP-1 and NDE1 associated with schizophrenia, to CMIs, offering fresh perspectives alongside genetics and environment as contributors to these conditions.

This thesis has set out to understand the complex process of protein aggregation in the context of schizophrenia. It aims to uncover the roles of TRIOBP-1 and NDE1 in co-aggregation, providing insights into how these proteins might relate to the condition. With growing evidence connecting protein aggregation to mental illnesses like schizophrenia, this thesis focuses on the interaction between TRIOBP-1 and NDE1, both essential players in cellular processes and neurobiology.

Recognizing NDE1's interactions with proteins that aggregate, such as TRIOBP-1 and DISC1, highlighted its significance in this context. We set out to confirm our ideas by verifying the co-aggregation of wild-type TRIOBP-1 and NDE1, using various methods to explore their complex relationships. We aimed to understand how NDE1's behaviour balances between stability and susceptibility to aggregation. EGFP's role in stabilizing NDE1, similar to CRMP1's effects, was intriguing. Unexpected findings, like the co-aggregation of Flag-NDE1 and EGFP, suggested NDE1's intricate binding capabilities. The discovery that NDE1 could trigger aggregation in mutant TRIOBP-1 echoed findings with DISC1. The insights from the insolubility assay indicated a combination of tubulin-bound and aggregating NDE1.

The intricate dynamics of protein interactions we've uncovered underscore the importance of continued research, holding the promise of revealing deeper insights into this enigmatic disorder and paving the way for hopeful developments in the future. The research on diagnosing and treating schizophrenia is at the forefront of medical progress. By delving into the complexities of protein aggregation and its link to this condition, we're moving closer to more precise diagnostics and innovative treatments. This effort reflects the commitment of science research to enhance the well-being of individuals with schizophrenia and holds promise for significant advancements in the field.

7. References

- 1 Sullivan PF, Geschwind DH. Defining the Genetic, Genomic, Cellular, and Diagnostic Architectures of Psychiatric Disorders. *Cell*. 2019; **177**: 162–183.
- 2 Institute of Health Metrics and Evaluation. Global Health Data Exchange (GHDx). <https://vizhub.healthdata.org/gbd-results/> (accessed 1 Sep2023).
- 3 NIMH » Mental Illness. National Institute of Mental Health. <https://www.nimh.nih.gov/health/statistics/mental-illness> (accessed 25 Jun2023).
- 4 Schizophrenia. World Health Organization. <https://www.who.int/news-room/fact-sheets/detail/schizophrenia> (accessed 25 Jun2023).
- 5 Ochoa S, Usall J, Cobo J, Labad X, Kulkarni J. Gender Differences in Schizophrenia and First-Episode Psychosis: A Comprehensive Literature Review. *Schizophr Res Treatment* 2012; **2012**: 1–9.
- 6 NIMH » Schizophrenia. <https://www.nimh.nih.gov/health/topics/schizophrenia> (accessed 26 Jun2023).
- 7 World Health Organization. The ICD-10 Classification of Mental and Behavioural Disorders Clinical descriptions and diagnostic guidelines World Health Organization. .
- 8 Kane JM, Correll CU. Pharmacologic treatment of schizophrenia. *Dialogues Clin Neurosci* 2010; **12**: 345.
- 9 Dixon L, McFarlane WR, Lefley H, Lucksted A, Cohen M, Falloon I *et al*. Evidence-Based Practices for Services to Families of People With

- Psychiatric Disabilities. <https://doi.org/10.1176/appi.ps527903> 2001; **52**: 903–910.
- 10 Wykes T, Reeder C, Landau S, Everitt B, Knapp M, Patel A *et al*. Cognitive remediation therapy in schizophrenia: Randomised controlled trial. *British Journal of Psychiatry* 2007; **190**: 421–427.
 - 11 Yanos PT, Primavera LH, Knight EL. Consumer-run service participation, recovery of social functioning, and the mediating role of psychological factors. *Psychiatric Services* 2001; **52**: 493–500.
 - 12 Drake RE, Mueser KT, Brunette MF, McHugo GJ. A Review of Treatments for People with Severe Mental Illnesses and Co-Occurring Substance Use Disorders. *Psychiatr Rehabil J* 2004; **27**: 360–374.
 - 13 Lehman AF, Lieberman JA, Dixon LB, McGlashan TH, Miller AL, Perkins DO *et al*. Practice Guideline for the Treatment of Patients with Schizophrenia, Second Edition. *American Journal of Psychiatry* 2004; **161**: i-iv+1-56.
 - 14 Van Erp TGM, Hibar DP, Rasmussen JM, Glahn DC, Pearlson GD, Andreassen OA *et al*. Subcortical brain volume abnormalities in 2028 individuals with schizophrenia and 2540 healthy controls via the ENIGMA consortium. *Mol Psychiatry* 2016; **21**: 547–553.
 - 15 Van den Heuvel MP, Mandl RCW, Scheeuwe T, Kahn W, Kahn RS, Pol HEH. Dysfunctional connectivity in schizophrenia. *World Psychiatry* 2002; **1**: 66.
 - 16 Kochunov P, Huang J, Chen S, Li Y, Tan S, Fan F *et al*. White matter in schizophrenia treatment resistance. *American Journal of Psychiatry* 2019; **176**: 829–838.
 - 17 Howes OD, Kapur S. The Dopamine Hypothesis of Schizophrenia: Version III—The Final Common Pathway. *Schizophr Bull* 2009; **35**: 549.

- 18 Coyle JT. NMDA Receptor and Schizophrenia: A Brief History. *Schizophr Bull* 2012; **38**: 920.
- 19 Munawar N, Ahsan K, Muhammad K, Ahmad A, Anwar MA, Shah I *et al*. Hidden role of gut microbiome dysbiosis in schizophrenia: Antipsychotics or psychobiotics as therapeutics? *Int J Mol Sci*. 2021; **22**. doi:10.3390/ijms22147671.
- 20 Talukdar PM, Abdul F, Maes M, Binu V, Venkatasubramanian G, Kutty BM *et al*. Maternal Immune Activation Causes Schizophrenia-like Behaviors in the Offspring through Activation of Immune-Inflammatory, Oxidative and Apoptotic Pathways, and Lowered Antioxidant Defenses and Neuroprotection. *Mol Neurobiol* 2020; **57**: 4345–4361.
- 21 Cheslack-Postava K, Brown AS. Prenatal infection and schizophrenia: A decade of further progress. *Schizophr Res* 2022; **247**: 7–15.
- 22 Hall MB, Willis DE, Rodriguez EL, Schwarz JM. Maternal immune activation as an epidemiological risk factor for neurodevelopmental disorders: Considerations of timing, severity, individual differences, and sex in human and rodent studies. *Front Neurosci*. 2023; **17**. doi:10.3389/fnins.2023.1135559.
- 23 Hilker R, Helenius D, Fagerlund B, Skytté A, Christensen K, Werge TM *et al*. Heritability of Schizophrenia and Schizophrenia Spectrum Based on the Nationwide Danish Twin Register. *Biol Psychiatry* 2018; **83**: 492–498.
- 24 Trubetskoy V, Pardiñas AF, Qi T, Panagiotaropoulou G, Awasthi S, Bigdeli TB *et al*. Mapping genomic loci implicates genes and synaptic biology in schizophrenia. *Nature* 2022; **604**: 502.
- 25 Wawrzczak-Bargieła A, Bilecki W, Maćkowiak M. Epigenetic Targets in Schizophrenia Development and Therapy. *Brain Sci* 2023; **13**: 426.

- 26 Bradshaw NJ, Korth C. Protein misassembly and aggregation as potential convergence points for non-genetic causes of chronic mental illness. *Molecular Psychiatry* 2018 24:7 2018; **24**: 936–951.
- 27 Scott MR, Meador-Woodruff JH. Intracellular compartment-specific proteasome dysfunction in postmortem cortex in schizophrenia subjects. *Mol Psychiatry* 2020; **25**: 776–790.
- 28 Stefani M. Protein misfolding and aggregation: new examples in medicine and biology of the dark side of the protein world. *Biochimica et Biophysica Acta (BBA) - Molecular Basis of Disease* 2004; **1739**: 5–25.
- 29 Taylor JP, Hardy J, Fischbeck KH. Toxic Proteins in Neurodegenerative Disease. *Science (1979)* 2002; **296**: 1991–1995.
- 30 Bradshaw NJ, Bader V, Prikulis I, Lueking A, Müllner S, Korth C. Aggregation of the Protein TRIOBP-1 and its potential relevance to schizophrenia. *PLoS One* 2014; **9**. doi:10.1371/journal.pone.0111196.
- 31 Seipel K, O'Brien SP, Lannotti E, Medley QG, Streuli M. Tara, a novel F-actin binding protein, associates with the Trio guanine nucleotide exchange factor and regulates actin cytoskeletal organization. *J Cell Sci* 2001; **114**: 389–399.
- 32 Shahin H, Walsh T, Sobe T, Abu Sa'ed J, Abu Rayan A, Lynch ED *et al*. Mutations in a novel isoform of TRIOBP that encodes a filamentous-actin binding protein are responsible for DFNB28 recessive nonsyndromic hearing loss. *Am J Hum Genet* 2006; **78**: 144–152.
- 33 Riazuddin S, Khan SN, Ahmed ZM, Ghosh M, Caution K, Nazli S *et al*. Mutations in TRIOBP, which encodes a putative cytoskeletal-organizing protein, are associated with nonsyndromic recessive deafness. *Am J Hum Genet* 2006; **78**: 137–143.

- 34 Bader V, Tomppa L, Trossbach S V., Bradshaw NJ, Prikulis I, Rutger Leliveld S *et al.* Proteomic, genomic and translational approaches identify CRMP1 for a role in schizophrenia and its underlying traits. *Hum Mol Genet* 2012; **21**: 4406.
- 35 Bradshaw NJ, Yerabham ASK, Marreiros R, Zhang T, Nagel-Steger L, Korth C. An unpredicted aggregation-critical region of the actinpolymerizing protein TRIOBP-1/Tara, determined by elucidation of its domain structure. *Journal of Biological Chemistry* 2017; **292**: 9583–9598.
- 36 Zaharija B, Odorčić M, Hart A, Samardžija B, Marreiros R, Prikulis I *et al.* TRIOBP-1 Protein Aggregation Exists in Both Major Depressive Disorder and Schizophrenia, and Can Occur through Two Distinct Regions of the Protein. *Int J Mol Sci* 2022; **23**. doi:10.3390/ijms231911048.
- 37 Juković M. Protein interaction partners of TRIOBP-1, and its effect on their aggregation in schizophrenia, Master's thesis. 2021.
- 38 Bakircioglu M, Carvalho OP, Khurshid M, Cox JJ, Tuysuz B, Barak T *et al.* The Essential Role of Centrosomal NDE1 in Human Cerebral Cortex Neurogenesis. *Am J Hum Genet* 2011; **88**: 523.
- 39 Bradshaw NJ, Hayashi MAF. NDE1 and NDEL1 from genes to (mal)functions: parallel but distinct roles impacting on neurodevelopmental disorders and psychiatric illness. *Cell Mol Life Sci* 2017; **74**: 1191–1210.
- 40 Sweeney KJ, Prokscha A, Eichele G. NudE-L, a novel Lis1-interacting protein, belongs to a family of vertebrate coiled-coil proteins. *Mech Dev* 2001; **101**: 21–33.
- 41 Hennah W, Tomppa L, Hiekkalinna T, Palo OM, Kilpinen H, Ekelund J *et al.* Families with the risk allele of DISC1 reveal a link between

- schizophrenia and another component of the same molecular pathway, NDE1. *Hum Mol Genet* 2007; **16**: 453–462.
- 42 Soto-Perez J, Baumgartner M, Kanadia RN. Role of NDE1 in the Development and Evolution of the Gyrified Cortex. *Front Neurosci* 2020; **14**. doi:10.3389/fnins.2020.617513.
- 43 Bradshaw NJ, Hennah W, Soares DC. NDE1 and NDEL1: twin neurodevelopmental proteins with similar 'nature' but different 'nurture'. *Biomol Concepts* 2013; **4**: 447–464.
- 44 Samardžija B, Juković M, Zaharija B, Renner É, Palkovits M, Bradshaw NJ. Co-Aggregation and Parallel Aggregation of Specific Proteins in Major Mental Illness. *Cells* 2023; **12**. doi:10.3390/cells12141848.
- 45 Agrotis A, Pengo N, Burden JJ, Ketteler R. Redundancy of human ATG4 protease isoforms in autophagy and LC3/GABARAP processing revealed in cells. *Autophagy* 2019; **15**: 976–997.
- 46 Hong JH, Kwak Y, Woo Y, Park C, Lee SA, Lee H *et al*. Regulation of the actin cytoskeleton by the Ndel1-Tara complex is critical for cell migration. *Sci Rep* 2016; **6**. doi:10.1038/srep31827.
- 47 Soares DC, Bradshaw NJ, Zou J, Kennaway CK, Hamilton RS, Chen ZA *et al*. The Mitosis and Neurodevelopment Proteins NDE1 and NDEL1 Form Dimers, Tetramers, and Polymers with a Folded Back Structure in Solution. *Journal of Biological Chemistry* 2012; **287**: 32381–32393.

Appendix

Enzymes, stains, and commercially prepared kits

Bio-Budget Technologies GmbH

QIAGEN

my-Budget DNA/RNA Stain Green

QIAprep Spin Miniprep Kit

Gels

Agarose gel (handmade)

Table 6: Measurements for agarose gel

Agarose	1x TAE buffer	DNA stain
0.5 g	50 mL	0.5 µL

Acrylamide running gel (handmade)

Table 7: Measurements for 8% and 10% acrylamide running gels

	dH₂O	30% acrylamide	1.5M Tris [pH 8.8]	10% SDS	10% APS	TEMED
8%	5.5 mL	3.2 mL	3 mL	120 µL	120 µL	12 µL
10%	4.8 mL	3.9 mL	3 mL	120 µL	120 µL	12 µL

Acrylamide stacking gel (handmade)

Table 8: Measurements for acrylamide stacking gel

dH₂O	30% acrylamide	1.0M Tris [8.6 pH]	10% SDS	10% APS	TEMED
2.6 mL	1.0 mL	625 µL	50 µL	50 µL	5 µL

Insoluble fraction purification buffers

Lysis Buffer for Protein Extraction: 50 mM HEPES [pH 7.5], 250 mM sucrose, 5 mM MgCl₂, 100 mM KAc (KCH₃COO), 2 mM PMSF, 1x Pi

A1: 50 mM HEPES [pH 7.5], 1.6 M sucrose, 100 mM KAc, 1% Triton-X-100, 1mM PMSF

B1: 50 mM HEPES [pH 7.5], 1M NaCl, 20 mM MgCl₂, 30 mM Ca²⁺, 100 U/mL DNaseI, 1x Pi

C1: 50 mM HEPES [pH 7.5], 0.5% sarcosyl

Note: PMSF and DNaseI should only be added immediately before use!

Buffers and solutions

Buffers and solutions used in this thesis were made in deionized distilled water (dH₂O) and are listed below, in alphabetical order.

30% acrylamide solution

14.6 g acrylamide

0.5 g *N,N'*-methylbisacrylamide

dH₂O up to 100 mL

Cell Fixing buffer

8 g Paraformaldehyde (PFA)

20 mL 10x PBS

dH₂O up to 200 mL

Set pH to 7.4

Cell Lysis buffer

5 mL 10x PBS (1x)

5 mL 10% Triton X-100 (1%)

1 mL 1M Magnesium chloride (MgCl₂)

dH₂O up to 50 mL

DMEM or DMEM-F12

500 mL DMEM or DMEM-F12
50 mL Fetal calf serum (FCS)
5 mL 100x penicillin/streptomycin solution
5 mL 100x non-essential amino acid solution

DNA Loading buffer

5 µL 10% SDS
80 0.25M EDTA
~ 5 mg bromophenol blue
dH₂O up to 50 mL

Fixation buffer

(PBS/4% paraformaldehyde)
8 g Paraformaldehyde (PFA)
20 mL 10x PBS
dH₂O up to 200 mL
Set pH to 7.4
Heat to 50°C and periodically
Add 1M NaOH to dissolve PFA

LB agar

1 g Tryptone
0.5 g Yeast extract
0.5 g NaCl
1.5 g Agar
dH₂O up to 100 mL

LB media

10 g Tryptone
5 g Yeast extract
5 g NaCl
dH₂O up to 1L
Sterilize by autoclaving!

PBS-Tween

100 mL 10x PBS
500 µL Tween-20
dH₂O up to 1 L

Permeabilization buffer

(PBS/Triton X-100)
10 mL 10% Triton X-100
10 mL 10x PBS
dH₂O up to 100 mL

Phosphate-buffered saline (PBS)

80 g NaCl
2 g KCl
14.4 g Na₂HPO₄
2.4 g KH₂PO₄
dH₂O up to 1 L
Set pH to 7.4

Ponceau S stain

1 g Ponceau S
4 mL acetic acid
dH₂O up to 200 mL

Protein loading buffer

6.25 1M Tris [pH 6.8]
10 mL Glycerol
20 mL 10% SDS
3.75 mL dH₂O
~ 5 mg Bromophenol blue

10x SDS-PAGE running buffer

30 g Tris
144 g glycine
10 g SDS
dH₂O up to 1 L

50x TAE buffer

242 g Tris
18.61 g EDTA
57.1 mL Acetic acid
dH₂O up to 1 L

TE buffer

0.5 mL 1M Tris [pH 7.4]
200 µL 0.25M EDTA
dH₂O up to 50 mL

Transfer buffer (1x)

5.8 g Tris
2.9 g Glycine
4 mL 10% SDS
200 mL Methanol
dH₂O up to 1 L

List of Figures and Tables

Figures

Figure 1: Schematic representation of misfolded protein fate.....	6
Figure 2: The predicted domain structure of TRIOBP-1.	10
Figure 3: The predicted domain structure of NDE1 and its interaction regions.....	13
Figure 4: Gateway LR Clonase recombination reaction scheme.....	20
Figure 5: Nocodazole structure.	28
Figure 6: Western blot analysis for anti-GFP and anti-Flag M2 stained membranes with constructs used in this thesis, expressed in HEK293T cells.....	31
Figure 7: Single transfection controls.....	33
Figure 8: Replicating previous research results in SH-SY5Y cells with fluorescent microscopy.....	34
Figure 9: Single transfection controls for the experiment of switching vectors in NDE1 and TRIOBP-1 observed in SH-SY5Y cells with fluorescent microscopy.	36
Figure 10: Switching vectors in NDE1 and TRIOBP-1 to observe the effect it has on the aggregation of those proteins in SH-SY5Y cells with fluorescent microscopy...	37
Figure 11: Ultracentrifugation assay revealed the insolubility of both single transfected TRIOBP-1 and NDE1, and their co-aggregates.....	40
Figure 12: The ultracentrifugation assay was performed after treating cells with nocodazole to assess its effect on the aggregome of NDE1 specifically.	42
Figure 13: Controls for expressing NDE1 and TRIOBP-1 plasmids in HEK293T.	44
Figure 14: Expressing NDE1 and TRIOBP-1 plasmids in HEK293T to check if aggregation propensity changes by changing a cell line.	45
Figure 15: NDE1 aggregates.	51
Figure 16: NDE1 molecules..	51
Figure 17: NDE1 co-expressed with EGFP control in HEK293T cell line.....	53

Tables

Table 1: List of expression and entry vectors	16
Table 2: List of primary and secondary antibodies, as well as nuclear and cytoskeletal stains used in Western blot and cell staining (immunocytochemistry)	17
Table 3: LR clonase reaction	21
Table 4: List of plasmids.....	29
Table 5: List of used and related plasmids and their tendency to aggregate when over-expressed	50
Table 6: Measurements for agarose gel.....	65
Table 7: Measurements for 8% and 10% acrylamide running gels	65
Table 8: Measurements for acrylamide stacking gel	65

Financial support

This research was supported by grants from the Croatian Science Foundation (HRZZ: Hrvatska zaklada za znanost): IP-2018-01-9424, "Istraživanje shizofrenije kroz ekspresiju netopivih proteina (ISkrEN)" and the Alexander von Humboldt Foundation: 1142747-HRV-IP, "DISC1: Its Structure, Aggregation and Relationship to Disease (DISCARD)."

Anja Hart

Date of birth: 11/07/1998 | **Nationality:** Croatian | **Gender:** Female | **Phone number:** (+385) 0996905487 (Mobile) |

Email address: anjahart5@gmail.com | **LinkedIn:** <https://www.linkedin.com/in/anja-hart-/> |

Address: Arslanovci 44, 34000, Požega, Croatia (Home)

● WORK EXPERIENCE

02/2023 – 08/2023 Vienna, Austria

ERASMUS+ INTERNSHIP MEDICAL UNIVERSITY OF VIENNA

Experimental lab work at the Center for Pathobiochemistry & Genetics (Institute of Medical Chemistry and Pathobiochemistry).

Learning major cell biology techniques as well as genetics approaches to decipher single-cell heterogeneity of human cancer cell responses to chemo-therapeutic pressure. Utilization of Celleste image analysis software and ImageJ for computational image analysis and employment of Excel and GraphPad Prism for statistical analysis.

10/2022 – 01/2023 Jülich, Germany

ERASMUS+ INTERNSHIP FORSCHUNGSZENTRUM JÜLICH

Experimental lab work at the Institute for Biological Information Processes (Structural Biochemistry).

Knowledge, skills and practical experience acquired in the fields of:

- Protein expression and purification (affinity chromatography, HPLC)
- Biophysical methods used in the characterisation of proteins (dynamic light scattering (DLS))
- Structural characterization using liquid-state nuclear magnetic resonance (NMR)
- Protein crystallisation for structure determination, data acquisition, processing, and visualisation in X-ray crystallography

06/2020 – 07/2020 Rijeka, Croatia

COMPULSORY INTERNSHIP DEPARTMENT OF BIOTECHNOLOGY, UNIVERSITY OF RIJEKA

DNA analysis techniques, PCR, ligation, plasmid cloning, isolation of DNA from TAE agarose gels

Part of a project: *Istraživanje shizofrenije kroz ekspresiju netopivih proteina (ISKREN), IP-2018-01-9424*

02/11/2018 – 23/12/2018 Rijeka, Croatia

STUDENT TEACHING ASSISTANT AT COURSE 'CELLULAR AND MOLECULAR BIOLOGY' DEPARTMENT OF BIOTECHNOLOGY, UNIVERSITY OF RIJEKA

Microscopy, chromosomal sex determination, karyotype, gametogenesis, isolation of genomic DNA

● EDUCATION AND TRAINING

10/2020 – 09/2023 RIJEKA, Croatia

MSC BIOTECHNOLOGY IN MEDICINE Department of Biotechnology, University of Rijeka

Address 51000, RIJEKA, Croatia

10/2017 – 09/2020 RIJEKA, Croatia

BSC BIOTECHNOLOGY AND DRUG RESEARCH Department of Biotechnology, University of Rijeka

Address 51000, RIJEKA, Croatia | **Thesis** Aggregation-resistant mutants of the schizophrenia-related protein TRIOBP-1

Link <https://zir.nsk.hr/islandora/object/biotechri%3A531>

2013 – 2017 POŽEGA, Croatia

NATURAL-SCIENCES AND MATHEMATICS PROGRAMME High school "Gymnasium Požega"

Address 34000, POŽEGA, Croatia

● LANGUAGE SKILLS

Mother tongue(s): **CROATIAN**

Other language(s):

	UNDERSTANDING		SPEAKING		WRITING
	Listening	Reading	Spoken production	Spoken interaction	
ENGLISH	C2	C2	C2	C2	C2
GERMAN	A2	A2	A2	A2	A2

Levels: A1 and A2: Basic user; B1 and B2: Independent user; C1 and C2: Proficient user

DIGITAL SKILLS

Microsoft Office

Microsoft Office: proficient user of Word, Excel and Powerpoint

Molecular design software

PyMOL, Avogadro, ChemAxon, Marvin, VMD, GAMESS, MacMOLPit | UCSF ChimeraX

Laboratory image analysis

Celleste Image Analysis Software | Image J (Laboratory Image Analysis)

Statistical analysis

GraphPad Prism

ADDITIONAL INFORMATION

PUBLICATIONS

[TRIOBP-1 Protein Aggregation Exists in Both Major Depressive Disorder and Schizophrenia, and Can Occur through Two Distinct Regions of the Protein](#)

– 2022

doi: 10.3390/ijms231911048

DRIVING LICENCE

Driving Licence: B

CONFERENCES AND SEMINARS

08/06/2022 – 10/06/2022 – Groningen, the Netherlands

Presenting participant at the International Student Congress Of (bio)Medical Sciences (ISCOMS) ISCOMS is one of the world's leading student congresses in (bio)medical sciences, it is a non-profit organisation that aims to promote student research and the international exchange of it.

At this conference, I gave a poster presentation titled "Aggregation of the protein TRIOBP-1m involved in schizophrenia, depends on two of its structural regions" and won a prize for the best presentation in the Cell biology category.

03/12/2021 – 04/12/2021 – International Virtual Conference

Darwin Regional Conference on Revolutionary Movements in Biology This is a global celebration of biology and research enthusiasts facilitated through a panel of experts sharing about cutting-edge research topics, talks by established biologists, virtual workshops, tours and the Research Symposium – a paper presentation competition. This year, the conference was centred around Cutting-Edge Biology with sub-themes: BioArt, Cell Biology and Medical Biology.

23/04/2021 – 25/04/2021 – Rijeka, Croatia / Online

Presenting participant at the Student Congress of Neuroscience (NeuRi) NeuRi is a student-organised conference where students and researchers engaged in scientific research within the rich neuroscience range, from neuroanatomy, neurophysiology, neuropharmacology through neurology and psychiatry to psychology and all other areas that study the human brain and its function, can present their work.

At the conference, I gave a presentation on my Bachelor's thesis research project titled "Investigating the mechanism of TRIOBP-1 aggregation in mental illness"

HONOURS AND AWARDS

05/2022

1st place in STEM games Science arena STEM Games manifestation is an international problem-solving competition for students in STEM fields.

Science Arena is aimed at students studying in the fields of Natural and Biotechnical Sciences and the corresponding fields and branches.

This year the topic of the Science arena was Oceanography. We used Excel and R Studio for the data analysis of oceanographic research data correlated with the understanding of the ecosystem for renewable development.

COMMUNICATION AND INTERPERSONAL SKILLS

Student jobs I improved my communication skills thanks to summer student jobs (work in shops and restaurants) where I have had the opportunity to work with many different people (customers and co-workers). Seasonal jobs have helped me become very diligent, adaptable and responsible. It is of great importance to me that this experience has allowed me to quickly adapt to different teams and therefore I am capable of teamwork, but I also like to work independently. I am open to new experiences.

VOLUNTEERING

10/2018 – 09/2023 Rijeka, Croatia

Student mentor Helping randomly assigned younger students of the Department of Biotechnology with academic questions at the very beginning and throughout the years with guidelines and tips on how to engage in academic and social events.

2017 – 2023 Rijeka, Croatia

Member of 'Biotechnology Student Association at University of Rijeka (USBRI)' A student-led organization at Department of Biotechnology, University of Rijeka that aims to promote life sciences.

ADVANCED TRAINING AND ADDITIONAL EDUCATION

06/2023

Image Processing with Python at Earlham Institute Norwich, UK

10/2021 – 06/2022

German Language at the Adult Education Institution 'Dante' level A1
